Journal of Medicinal Chemistry

Article

pubs.acs.org/jmc

Conformational Restriction and Enantioseparation Increase Potency and Selectivity of Cyanoguanidine-Type Histamine H_4 Receptor Agonists

Roland Geyer, Uwe Nordemann, Andrea Strasser, Hans-Joachim Wittmann, and Armin Buschauer*

Institute of Pharmacy, Pharmaceutical/Medicinal Chemistry, Faculty of Chemistry and Pharmacy, University of Regensburg, Universitätsstraße 31, D-93053 Regensburg, Germany

Supporting Information

ABSTRACT: 2-Cyano-1-[4-(1*H*-imidazol-4-yl)butyl]-3-[2-(phenylsulfanyl)ethyl]guanidine (UR-PI376, **1**) is a potent and selective agonist of the human histamine H_4 receptor (hH_4R). To gain information on the active conformation, we synthesized analogues of **1** with a cyclopentane-1,3-diyl linker. Affinities and functional activities were determined at recombinant hH_xR (*x*: 1−4) subtypes on Sf9 cell membranes (radioligand binding, [^{35}S]GTPγS, or GTPase assays) and in part in luciferase assays on human or mouse H_4R (HEK-293 cells). The most potent H_4R agonists among 14 racemates were separated by chiral HPLC, yielding eight enantiomerically pure compounds. Configurations were assigned based on X-ray structures of intermediates and a stereocontrolled synthetic pathway. (+)-2-Cyano-1-{[*trans*-(1*S*,3*S*)-3-(1*H*-imidazol-4-yl)cyclopentyl]methyl}-3-[2-(phenylsulfanyl)ethyl]guanidine ((1*S*,3*S*)-UR-RG98, **39a**) was the most potent H_4R agonist in this series (EC_{50} 11 nM; H_4R vs H_3R, >100-fold selectivity; H_1R, H_2R, negligible activities), whereas the optical antipode proved to be an H_4R antagonist ([^{35}S]GTPγS assay). MD simulations confirmed differential stabilization of the active and inactive H_4R state by the enantiomers.

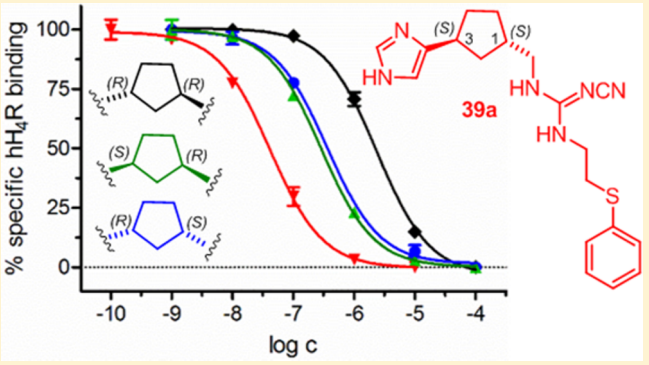

INTRODUCTION

In 2000 and 2001, the human histamine H_4 receptor (hH_4R) was identified and cloned, independently by several research groups, due to its rather high sequence homology with the hH_3R.[1−7] The H_4R is expressed in various cells of the immune system, suggesting a role in inflammatory, autoimmune, and allergic disorders.[8−16] Hence, the H_4R is considered as a promising drug target for the treatment of, e.g., allergic rhinitis, rheumatoid arthritis, bronchial asthma, and pruritus.[8,10−13,17−24] Regardless of that, there are controversial results published, for example, regarding the expression of functional H_4Rs in monocytes and in the brain[16,25−27] and species-dependent discrepancies regarding potencies, receptor selectivities, and even opposite qualities of action of H_4R ligands are reported, in part depending on the assay used.[28−36] Whereas H_4R antagonists are of potential therapeutic value, agonists are considered as molecular tools. In the case of imidazole-type compounds, which are reminiscent of the endogenous agonist, receptor subtype selectivity proved to be a critical issue, especially concerning the discrimination between the H_4R and the H_3R.[18,21]

The aim of the present study was to gain information on the stereochemical requirements of imidazole-type H_4R agonists. Cyanoguanidines such as 2-cyano-1-[4-(1*H*-imidazol-4-yl)-butyl]-3-[2-(phenylsulfanyl)ethyl]guanidine (UR-PI376 **1**),[37] derived from imbutamine (**2**),[38,39] and a derivative of imifuramine (**3**),[40,41] 1-{[(2*R*,5*R*)-5-(1*H*-imidazol-4-yl)-tetrahydrofuran-2-yl]methyl}-2-cyano-3-methylguanidine (OUP-16, **4**),[42] were reported as potent histamine H_4R agonists (Figure 1). Compared to the corresponding primary amines **2** and **3**, which are hH_3R preferring agonists, the introduction of the nonbasic cyanoguanidine moiety shifted the selectivity toward the H_4R. However, residual activity at the H_3R subtype is still a drawback of these and other imidazole-type H_4R ligands.[18] Watanabe et al.[43] identified conformationally restricted histamine analogues comprising a cyclopropane moiety (cf. Figure 1) as H_3R and/or H_4R antagonists with a pharmacological profile depending on the stereochemistry. In the case of imifuramine-type amines, all stereoisomers were partial to full agonists with preference for the hH_3R. By contrast, both potency and intrinsic activity increased in favor of the hH_4R by introduction of a nonbasic cyanoguanidine moiety.[42] Compound **4** was reported as a full hH_4R agonist with 40-fold selectivity over the hH_3R and superior to its (2*S*,5*S*)-configured optical antipode.[42] In the case of **1**, bulky substituents such as phenylsulfanylethyl at the cyanoguanidine group were superior to smaller residues such as methyl to increase the H_4R selectivity.[37]

Received: January 25, 2016

DOI: 10.1021/acs.jmedchem.6b00120
J. Med. Chem. XXXX, XXX, XXX−XXX

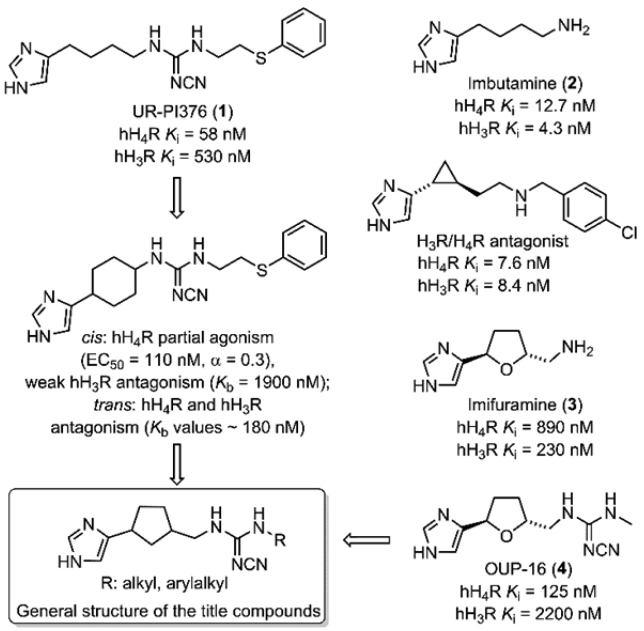

Figure 1. Selected imidazole-type histamine H_4R ligands, reported pharmacological data,[37,38,42−44] and general structure of the title compounds.

In a first attempt to optimize the structure of H_4R agonists derived from **1**, we introduced carbocycles instead of a flexible chain.[44] A phenylene spacer proved to be inappropriate, whereas a cyclohexylene linker was tolerated. This prompted us to further explore conformational constraints by analogy with the approach reported for compound **4**. Aiming at imidazole-type H_4R agonists with improved selectivity and taking into consideration that substances with reduced flexibility and defined stereochemistry might help to refine H_4R−ligand interaction models, we designed a series of compounds with a cyclopentane-1,3-diyl linker, combining structural features of **1** and **4** (Figure 1). In the following, the preparation of potent and selective hH_4R agonists including chiral separation, assignment of the absolute configuration based on crystal structures of intermediates and stereoselective synthesis is reported. Pharmacological characterization was performed by functional assays and radioligand binding studies on human histamine receptor subtypes. Additionally, MD simulations of two selected entantiomers, docked into the inactive and active state models of hH_4R, were performed in order to explain the experimental data on a molecular level.

RESULTS AND DISCUSSION

Chemistry. The *cis*- and *trans*-configured imidazolylcyclopentylmethylcyanoguanidines **31**−**42** and **46**−**47** were synthesized as racemic mixtures in 11 steps starting from norbornene (**5**) (Scheme 1). *cis*-Selective oxidation of **5** yielded norcamphoric acid (**6**),[45] subsequent reduction with borane[46] gave the diol **7**,[46,47] and monoprotection with a *tert*-butyldiphenylsilyl group resulted in a racemic mixture of **8** and *ent*-**8** (not depicted). Swern oxidation[48] of the alcohol gave the aldehyde **9**. In this reaction epimerization occurred, giving two pairs of enantiomers. The diasteriomeric mixture **9** was treated with tosylmethyl isocyanide[49] (TosMIC) followed by ammonia in methanol, affording the corresponding imidazoles **10**. After protection of the imidazole nitrogen with a trityl group, the alcohol **11** was converted to the phthalimide **12**

Scheme 1. Synthesis of the Cyanoguanidines *cis*- and *trans*-31−42, -46, and -47 as Racemic Mixtures[a]

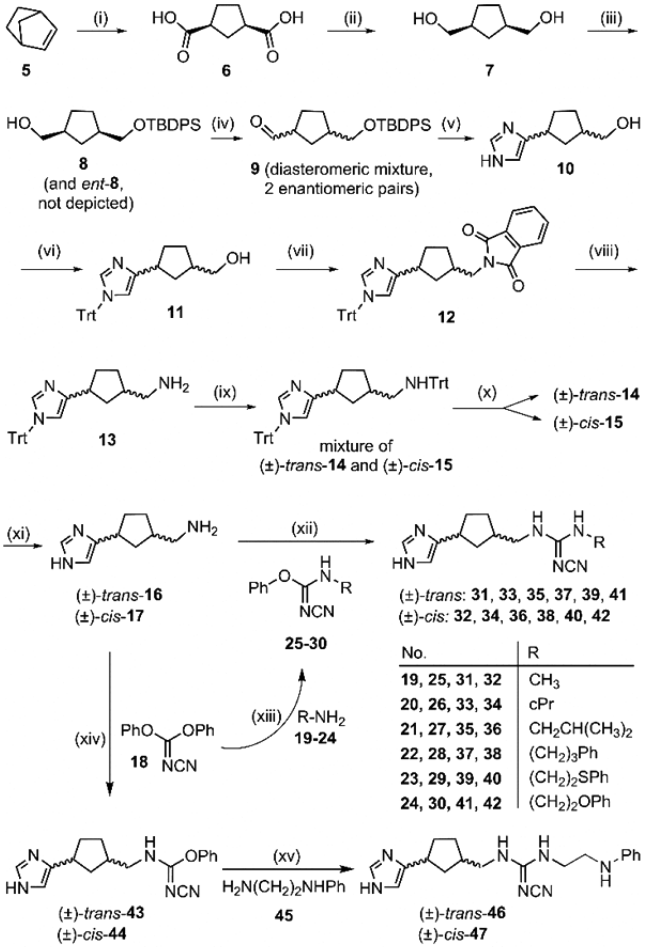

[a]Reagents and conditions: (i) $RuCl_3$ (2.2 mol %), $NaIO_4$ (4.1 equiv), EtOAc/MeCN/water 2:2:3, 2 d, rt, 99%. (ii) BH_3·THF (4.5 equiv), THF, 12 h, 0 °C → rt, 80%. (iii) TBDPSCl (0.98 equiv), DIPEA, DCM, 15 h, 0 °C → rt, 57%. (iv) DMSO (4 equiv), NEt_3 (8 equiv), $(COCl)_2$ (2 equiv), DCM, 3 h, −78 °C → 12 h, rt, 92%. (v) (a) TosMIC (1 equiv), NaCN (0.15 equiv), EtOH, 30 min, 0 °C; (b) 7 M NH_3 in MeOH, 18 h, 100 °C, 78%. (vi) TrtCl (1 equiv), NEt_3 (2 equiv), DMF, 24 h, rt, 83%. (vii) phthalimide (1.1 equiv), PPh_3 (1.1 equiv), DIAD (1.1 equiv), THF, overnight, 0 °C → rt, 75%, diasteriomeric ratio *trans*-**12**:*cis*-**12** = 58:42 (determined by ^1H NMR). (viii) N_2H_4·H_2O (5 equiv), EtOH, 1.5 h at reflux →1 h at rt, 92%. (ix) TrtCl (1.5 equiv), NEt_3 (2 equiv), DCM, 24 h, rt, 95%. (x) Separation of diastereomers by flash chromatography on silica gel, PE/EtOAc/7 M NH_3 in MeOH, 100/0/0−70/27/3 v/v/v), 80%. (xi) 37% HCl, MeOH, 3 h, reflux, ion exchanger, 88%. (xii) MeCN, microwave 150 °C, 15 min, 59−95%. (xiii) 2-propanol, 1 h, rt, 94%. (xiv) 2-propanol, 1 h, rt, 86−97%. (xv) MeCN, microwave 150 °C, 15 min, 55−69%.

under Mitsunobu conditions[50] and subsequent hydrazinolysis gave the primary amine **13**. Coupling of an additional trityl group to the primary amino group in **13** allowed for separation of the diastereomers **14** and **15** by flash chromatography. Deprotection under acidic conditions and conversion to the free bases with the help of an ion exchanger gave the racemic *cis*- and *trans*-configured amines **16** and **17**. The cyanoguanidines **31**−**42**, and **46**−**47** were synthesized by analogy with a previously described procedure[37,51] from diphenyl cyanocarbonimidate (**18**)[52] (Scheme 1). Compound **18** is prone to undergo 2-fold aminolysis when treated with one equivalent of

DOI: 10.1021/acs.jmedchem.6b00120
J. Med. Chem. XXXX, XXX, XXX−XXX

an ethylenediamine derivative such as **45**, resulting in the corresponding imidazole derivative.[53] Therefore, for the synthesis of **46**–**47**, the coupling steps were carried out in reversed order: the amines **16** and **17** were first allowed to react with **18** to give the isoureas **43** and **44**, which were subsequently treated with the aliphatic amine **45**.

Enantioseparation of Selected Racemates. On the basis of the pharmacological data determined for the pairs of racemic cyanoguanidines and taking into account the reported stereoselectivity of tetrahydrofuran-type compounds such as **3** and **4**,[42] the separation of the most promising racemates by chiral separation by HPLC was explored. Enantioseparation of the racemates **31**, **32**, **39**, and **40** was successful by analytical HPLC on a Chiralcel OJ-H column, using heptane/2-propanol as eluent and isocratic elution (Figure 2).

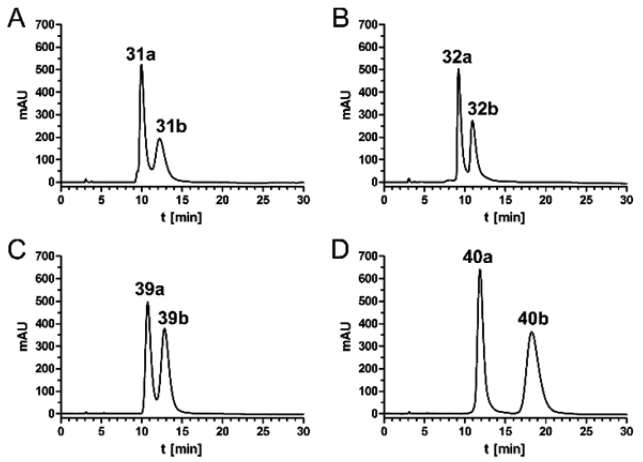

Figure 2. Analytical separation of the racemates on a Chiralcel OJ-H column (5 μm). (A) **31**; (B) **32**; eluent heptane/2-propanol 85/15; (C) **39**; (D) **40**, eluent heptane/2-propanol 80/20; flow, 1 mL/min; temperature, 30 °C, UV detection at 215 nm.

The optimized analytical HPLC method was applied for the separation of the enantiomers on a semipreparative scale (10–20 mg per injection) using a Chiralcel OJ-H column (5 μm, 20 mm × 250 mm). In case of incomplete enantioseparation after one run, the whole procedure was repeated. The enantiomeric excess, determined by peak integration, was >95%. The circular dichroism (CD) of the individual enantiomers was determined at 240 nm using a CD detector directly coupled to the HPLC system (Figure 3; Table 1). The separated enantiomers were numbered **a** and **b** according to the order of their elution. The stereochemical descriptors *R* and *S* given in Table 1 are based on the assignment of the absolute configurations as outlined below.

Determination of the Absolute Configuration. Attempts to crystallize the cyanoguanidines for X-ray analysis failed. Therefore, aiming at elucidation of the absolute configuration of the title compounds, a stereoselective synthesis was developed (Scheme 2) which selectively provided one *cis* and one *trans* enantiomer of the pertinent amine building block with known absolute configuration for conversion to the corresponding cyanoguanidines. Comparison of the optical rotation and HPLC data of these products with the data collected for the chromatographically separated enantiomers allowed unequivocal assignment of the absolute configuration of all investigated stereoisomers.

The key step of this approach was an enzymatic cleavage enabling the discrimination between the enantiotopic ester groups in meso-*cis*-cyclopentane-1,3-dicarboxylic acid dimethyl ester (**48**) according to the method published by Chênevert et al.[54] Dicarboxylic acid **6** was esterified with methanol in the presence of an acidic resin as catalyst to give **48** (Scheme 2). According to a reported procedure,[55] compound **48** was subjected to enzymatic cleavage by cholesterol esterase (CE), yielding the monoester (1*S*,3*R*)-**49** in 89% yield with 72% ee. The racemate (1*R**,3*S**)-**49**, obtained by dehydration of **6** with acetic anhydride followed by reaction of the anhydride, (1*R*,5*S*)-3-oxabicyclo[3.2.1]octane-2,4-dione[56] (**50**), with methanol, was used as a reference compound to assign the

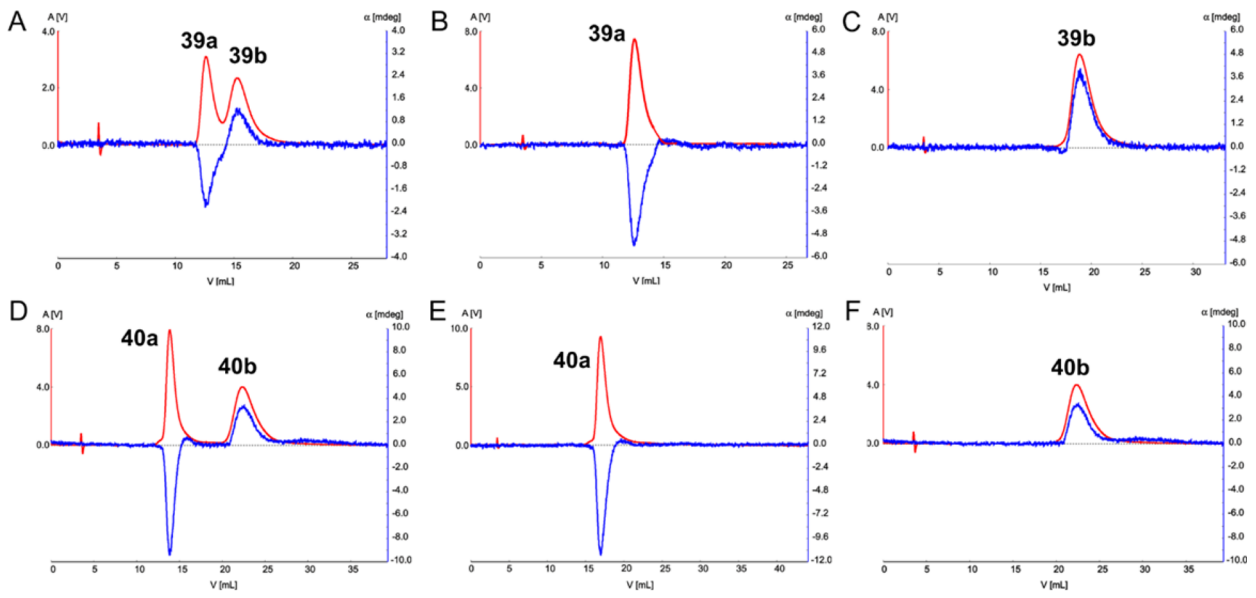

Figure 3. Enantioseparation by chiral HPLC using UV and CD detection. Chiralcel OJ-H column (5 μm), red, UV absorption at 240 nm; blue, circular dichroism at 240 nm. Concentration 1 mg/mL; heptane:2-propanol 80/20; flow, 0.5 mL/min; temperature, 25 °C. (A) Racemic *trans*-**39**, (B,C) chromatograms of purified **39a** and **39b**, (D) racemic *cis*-**40**, (E,F) chromatograms of purified **40a** and **40b**.

DOI: 10.1021/acs.jmedchem.6b00120
J. Med. Chem. XXXX, XXX, XXX–XXX

Table 1. Stereochemical Descriptors, Chromatographic Data, Enantiomeric Purity, CD, and Optical Rotation of the Separated Enantiomers 31a−32b and 39a−40b

								$[\alpha]^{25}$, [deg cm^3 dm^{-1} g^{-1}][f]		
no.[a]	stereochemical descriptors	R_S[b]	α[c]	t_R [min]	k'	ee[d] [%]	CD[e]	589 nm	546 nm	365 nm
31a	*trans*-(−)-(1*R*,3*R*)	1.23	1.33	9.85	2.26	98	+	−1.9	−2.3	−4.9
31b	*trans*-(+)-(1*S*,3*S*)			12.16	3.03	96	−	+1.7	+2.1	+6.1
32a	*cis*-(−)-(1*S*,3*R*)	1.23	1.27	9.11	2.01	>99	−	−21.0	−25.0	−44.6
32b	*cis*-(+)-(1*R*,3*S*)			10.83	2.59	97	+	+20.9	+23.9	+39.1
39a	*trans*-(+)-(1*S*,3*S*)	1.23	1.27	11.66	2.86	>99	−	+0.4	+0.45	+1.2
39b	*trans*-(−)-(1*R*,3*R*)			12.76	3.23	96	+	−1.0	−1.2	−3.8
40a	*cis*-(−)-(1*S*,3*R*)	2.67	1.72	11.83	2.92	>99	−	−16.2	−19.3	−34.1
40b	*cis*-(+)-(1*R*,3*S*)			20.32	5.72	97	+	+15.7	+18.8	+33.5

[a]**a** and **b** were assigned according to the order of elution of the corresponding enantiomers in chiral HPLC. [b]R_S = resolution of HPLC peaks; injection: 10 μL of a 1 mg/mL solution. [c]α = selectivity factor (k'_b/k'_a). [d]Enantiomeric excess. [e]Circular dichroism at 240 nm. [f]Optical rotation measured at the following compound concentrations (g/100 mL), **31a**, c 1.0, MeOH; **31b**, c 0.75, MeOH; **32a**, c 0.7, MeOH; **32b**, c 0.66, MeOH; **39a**, c 2.9, MeOH; **39b**, c 2.4, MeOH; **40a**, c 2.8, MeOH; **40b**, c 4.0, MeOH.

Scheme 2. Stereo-Controlled Synthetic Pathway to Assign the Configuration of the Enantiomers of Cyanoguanidines 31, 32, 39, and 40[a]

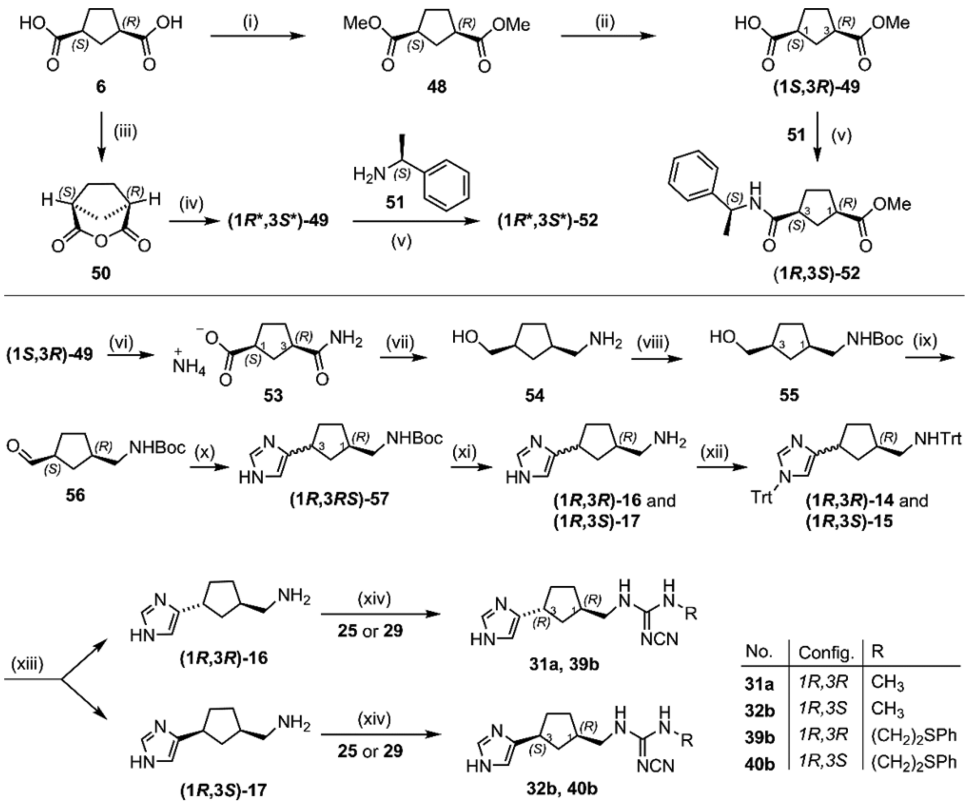

[a]Reagents and conditions: (i) Dowex 50x8 H^+-resin, MeOH, 12 h, reflux, 88%. (ii) cholesterol esterase (4000 U), 1 M NaOH, 0.05 M phosphate buffer pH 7.0, 1% MeCN, 37 °C, 89%, ee 72%. (iii) acetic anhydride, microwave, 150 °C, 30 min, 73%. (iv) MeOH, reflux, 4 h, 99%. (v) (a) DCM_{abs}, EDC, DMAP, 0 °C, 30 min; (b) **51**, rt, overnight, 92%. (vi) 32% $NH_{3(aq)}$, overnight, rt, 100%. (vii) BH_3·THF (4.5 equiv), THF, 1 h, 0 °C → rt, overnight, reflux, 70%. (viii) Boc_2O (1.1 equiv), 1 M NaOH, dioxane/water 2/1 (v/v), overnight, 0 °C → rt, 74%. (ix) DMSO (4 equiv), NEt_3 (8 equiv), $(COCl)_2$ (2 equiv), DCM, 3 h, −78 °C → 12 h, rt, 61%. (x) (a) TosMIC (1 equiv), NaCN (0.15 equiv), EtOH, 30 min, 0 °C; (b) 7 M NH_3 in MeOH, 18 h, 100 °C, 87%. (xi) 37% HCl, MeOH, overnight, rt, ion exchanger, 88%. (xii) TrtCl (6 equiv), NEt_3 (10 equiv), DCM, 24 h, rt, 80%. (xiii) (a) separation of diastereomers by flash chromatography on silica gel, PE/EtOAc/7 M NH_3 in MeOH, 100/0/0−70/27/3 v/v/v), 80%, diasteriomeric ratio *trans*:*cis* = 44:56; (b) 37% HCl, MeOH, 3 h, reflux, ion exchanger, 95−98%. (xiv) MeCN, microwave 150 °C, 15 min, 59−76%.

NMR data. The configuration of (1*S*,3*R*)-**49** was assigned by comparison of the specific optical rotation with reported values.[57] The enantiomeric purity of (1*S*,3*R*)-**49** was determined by derivatization with (*S*)-1-phenylethanamine (**51**) and ^{1}H NMR (600 MHz) analysis of the resulting diastereomeric amides **52**.

Compound (1*S*,3*R*)-**49** was treated with aqueous ammonia at room temperature to give the ammonium salt of the dicarboxylic acid monoamide (1*S*,3*R*)-**53**.[54] The absolute configuration of **53** was confirmed by X-ray diffraction analysis (Figure 4A). Reduction of **53** with borane[46,47] yielded the amino alcohol **54**. Boc-protection of the amine and subsequent

DOI: 10.1021/acs.jmedchem.6b00120
J. Med. Chem. XXXX, XXX, XXX−XXX

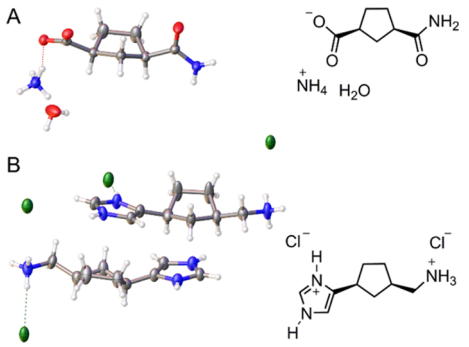

Figure 4. X-ray crystal structures. (A) *cis*-(1*R*,3*S*)-**53**·H_2O; (B) *cis*-(1*R*,3*S*)-**17**·2HCl; cf. Cambridge Crystallographic Data Center, CCDC 965185 and CCDC 965186.

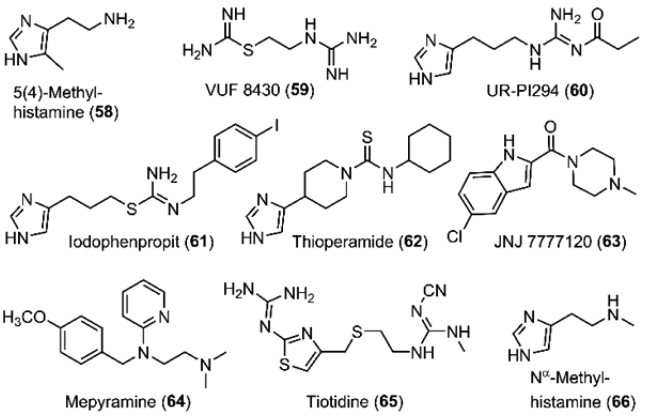

Figure 5. Structures of reference histamine receptor ligands **58**–**66** used for the pharmacological characterization of the title compounds (cf. Tables 2 and 3).

Swern oxidation[48] of **54** gave the corresponding aldehyde **56**. The imidazole ring was introduced according to the TosMIC ring closure procedure.[49] Under the basic conditions in this reaction, epimerization took place at the stereogenic center connected with the imidazole ring. By analogy with the procedure described in Scheme 1, the Boc group in (1*R*,3*RS*)-**57** was cleaved off, the imidazole nitrogen and the amino group were trityl-protected, and the diastereomers (1*R*,3*R*)-**14** and (1*R*,3*S*)-**15** were separated by flash chromatography. Deprotection under acidic conditions and conversion of the salts to the free bases with the help of a basic ion exchanger gave the *trans*-(1*R*,3*R*)- and *cis*-(1*R*,3*S*)-configured enantiomers of the imidazolylcyclopentylmethylamines **16** and **17**, respectively. Compound *cis*-(1*R*,3*S*)-**17** was crystallized as hydrochloride, and the configuration was confirmed by X-ray analysis (Figure 4B). The primary amines were converted to the corresponding *trans*-(1*R*,3*R*)- and *cis*-(1*R*,3*S*)-configured cyanoguanidines **31a**, **32b**, **39b**, and **40b** according to the method described above.

The approach summarized in Scheme 2 gave only small amounts of enantiomerically pure cyanoguanidines for analytical purposes. However, the absolute configuration of all pharmacologically characterized enantiomers (**31a**, **31b**, **32a**, **32b**, **39a**, **39b**, **40a**, **40b**) could be easily assigned by comparing optical rotation and chromatographic data (cf. Table 1) of the subset of cyanoguanidines prepared via stereoselective synthesis with those of the enantiomers separated in larger amounts by chiral HPLC.

Pharmacological Investigations. The amine precursors and the synthesized cyanoguanidines were investigated for agonism and antagonism at the hH_2R, hH_3R, and hH_4R subtypes in [^{35}S]GTPγS binding assays using membrane preparations of Sf9 insect cells coexpressing the hH_4R plus $G\alpha_{i2}$ plus $G\beta_1\gamma_2$ or the hH_3R plus $G\alpha_{i2}$ plus $G\beta_1\gamma_2$ or expressing the hH_2R-$Gs\alpha_s$ fusion protein. For the characterization of the compounds at the hH_1R, steady-state GTPase assays and radioligand binding experiments were performed using membrane preparations of Sf9 insect cells coexpressing the hH_1R plus RGS4. Additionally, selected compounds were investigated for agonism in luciferase reporter gene assays on human and mouse H_4R expressed in HEK-293 cells. The histamine receptor ligands depicted in Figure 5 (**58**,[38] **59**,[58] **60**,[59,60] **61**, **62**, **63**,[22] **64**–**66**) were used in nonlabeled or tritiated form as reference compounds and pharmacological tools for functional and binding studies.

Functional Activities of the Racemates at the H_xR Subtypes. The racemic amine precursors **16** and **17**, the carba analogues of **3**, were devoid of significant activity at the H_1R and the H_2R but were moderate H_4R partial agonists and H_3R antagonists (Table 2). The *cis*-configured amine **17** was the preferred diastereomer at both receptor subtypes. However, compared to the flexible analogue imbutamine[38] and the endogenous agonist histamine, efficacy and potency were drastically reduced by the introduction of the conformationally restricted linker.

In accordance with previous structure–activity relationship studies on imidazole-type H_4R ligands,[37,42] the replacement of an amino group by a nonbasic structural motif, the cyanoguanidine moiety, retained the H_4R affinity and, depending on substitution pattern and stereochemistry, increased the H_4R selectivity. Most of the investigated racemates revealed partial to full agonism at the H_4R with intrinsic activities (α) in the range from 0.40 to 0.94. Only three compounds, the *cis*-phenoxyethyl- and the two phenylaminoethyl-substituted cyanoguanidines, showed antagonistic (**42**, **46**) or inverse agonistic (**47**) activity. The K_B values for **42** and **46** were in the two-digit nanomolar range at the H_4R, whereas **47**, the *cis*-isomer of **46**, was virtually inactive (K_B > 10000 nM). The K_B values of these compounds at the H_3R were in the range of 400 nM. All the other racemates activated the H_4R with EC_{50} values ranging from 14 to 500 nM. In general, more bulky substituents compared to methyl provided higher potency at the H_4R. For instance, the isobutyl derivative **35** had an EC_{50} of 15 nM. Interestingly, unlike **32**, all racemic cyanoguanidines bearing substituents other than methyl showed higher agonist activity when *trans*-configured. Similar to the imidazolylbutylcyanoguanidine series,[37] phenylsulfanylethyl substitution at the cyanoguanidine was most favorable. Highest H_4R agonistic potency was achieved with the *trans*-configured derivative **39** (EC_{50} = 14 nM, α = 0.9). At the H_3R, compounds bearing alkyl residues at the cyanoguanidine moiety were weak partial agonists. With EC_{50} values from 370 to >10000 nM, these compounds showed some selectivity for the H_4R over the H_3R but no improved activities compared to flexible imidazolylbutylcyanoguanidines such as **1** or tetrahydrofurans such as **4**. Similar to **1** and in contrast to **4**,[42] compounds bearing an aromatic substituent (**37**–**42**, **46**–**47**) were devoid of agonistic activity at the H_3R. Compound **38** was the most potent H_3R antagonist with a K_B value of 70 nM. Both phenylsulfanylethyl-substituted cyanoguanidines, **39** and **40**, were moderate H_3R inverse agonists (α = −0.4 and −0.34). Contrary to the H_4R, the H_3R preferred the *cis*-configured isomers of most compounds. No agonistic

DOI: 10.1021/acs.jmedchem.6b00120
J. Med. Chem. XXXX, XXX, XXX–XXX

Table 2. Pharmacological Data of the Racemic Amines (16, 17) and Cyanoguanidines (31−42, 46, 47) and the Reference Compounds 1, 58−60, 62, and 63 at Human Histamine Receptor Subtypes, Determined in the [^{35}S]GTPγS Assay[a], the GTPase Assay,[b] or in Radioligand Binding Experiments[c,d]

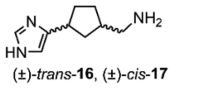

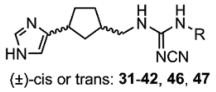

No.	Config.	R	No.	Config.	R
31	trans	CH_3	**38**	cis	$(CH_2)_3Ph$
32	cis	CH_3	**39**	trans	$(CH_2)_2SPh$
33	trans	cPr	**40**	cis	$(CH_2)_2SPh$
34	cis	cPr	**41**	trans	$(CH_2)_2OPh$
35	trans	$CH_2CH(CH_3)_2$	**42**	cis	$(CH_2)_2OPh$
36	cis	$CH_2CH(CH_3)_2$	**46**	trans	$(CH_2)_2NHPh$
37	trans	$(CH_2)_3Ph$	**47**	cis	$(CH_2)_2NHPh$

	hH_1R[e]		hH_2R		hH_3R		hH_4R	
compd	EC_{50} or (K_B), nM	N	EC_{50} or (K_B), nM	N	EC_{50} or (K_B), nM	N	EC_{50} or (K_B), nM	N
histamine	190 ± 8[f]		1410 ± 210[g]		13 ± 2	3	11 ± 3	3
	α: 1.0		α: 1.0		α: 1.0		α: 1.0	
1	(>10000)[h]		(>10000)[h]		720 ± 38	2	37 ± 3	3
	α: 0[I]		α: 0[I]		α: −0.52 ± 0.05		α: 0.88 ± 0.08	
16	na	2	>10000	2	(103 ± 0.5)	2	1710 ± 14	2
	α: 0[I]		α: 0[I]		α: 0[I]		α: 0.38 ± 0.01	
17	na	2	>10000	2	(62 ± 10)	2	150 ± 23	2
	α: 0.11 ± 0.06		α: 0.19 ± 0.10		α: 0[I]		α: 0.36 ± 0.01	
31	na	2	(>10000)	2	370 ± 6	2	206 ± 12	2
	α: 0[I]		α: 0[I]		α: −0.46 ± 0.06		α: 0.74 ± 0.05	
	K_i: >10000	2	K_i: nd		K_i: 830 ± 34	2	K_i: 240 ± 15	4
32	na	2	(>10000)	2	547 ± 55	2	111 ± 17	2
	α: 0[I]		α: 0[I]		α: 0.51 ± 0.02		α: 0.94 ± 0.01	
	K_i: >10000	2	K_i: nd		K_i: 860 ± 48	2	K_i: 155 ± 25	4
33	na	2	(>10000)	2	>10000	2	230 ± 62	2
	α: 0[I]		α: 0[I]		α: 0.36 ± 0.03		α: 0.74 ± 0.07	
34	na	2	(>10000)	2	1530 ± 14	2	245 ± 78	2
	α: 0[I]		α: 0[I]		α: 0.28 ± 0.09		α: 0.64 ± 0.02	
35	na	2	(>10000)	2	578 ± 13	2	15 ± 3	2
	α: 0[I]		α: 0[I]		α: 0.54 ± 0.04		α: 0.84 ± 0.07	
36	na	2	(>10000)	2	858 ± 68	2	202 ± 66	2
	α: 0[I]		α: 0[I]		α: 0.50 ± 0.00		α: 0.81 ± 0.07	
37	na	2	(>10000)	2	(325 ± 135)	2	125 ± 39	2
	α: −0.19 ± 0.17		α: 0[I]		α: −0.19 ± 0.02		α: 0.70 ± 0.05	
38	na	2	(>10000)	2	(70 ± 7)	2	372 ± 63	2
	α: 0[I]		α: 0[I]		α: 0[I]		α: 0.40 ± 0.11	
39	na	2	(>10000)	2	(246 ± 49)	2	14 ± 3	3
	α: 0[I]		α: 0[I]		α: −0.40 ± 0.05		α: 0.90 ± 0.06	
	K_i: 6080 ± 270	2	K_i: nd		K_i: 1230 ± 134	2	K_i: 99 ± 8	4
40	na	2	(>10000)	2	(162 ± 3)	2	129 ± 10	4
	α: 0[I]		α: 0[I]		α: −0.34 ± 0.04		α: 0.72 ± 0.09	
	K_i: 3800 ± 700	2	K_i: nd		K_i: 1350 ± 165	2	K_i: 250 ± 20	4
41	na	2	(>10000)	2	(540 ± 50)	2	524 ± 8	3
	α: 0[I]		α: 0[I]		α: 0[I]		α: 0.63 ± 0.10	
42	na	2	(>10000)	2	(328 ± 38)	2	(97 ± 7)	3
	α: 0[I]		α: 0[I]		α: 0[I]		α: 0[I]	
46	na	2	(>10000)	2	(408 ± 21)	2	(53 ± 6)	3
	α: 0[I]		α: 0[I]		α: 0[I]		α: 0.19 ± 0.01	
47	na	2	(>10000)	2	(402 ± 38)	2	(>10000)	3
	α: 0[I]		α: 0[I]		α: 0[I]		α: −0.40 ± 0.20	
58	16000 ± 540[h]		2900 ± 12[h]		12400 ± 3130[j]		70.3 ± 44.1[j]	
	α: 0.9		α: 1.0		α: 0.7		α: 0.9	
59	nd		nd		170 ± 11	3	44 ± 8	3
	α: nd		α: nd		α: 0.64 ± 0.07		α: 0.81 ± 0.03	
60	3467[k]		372[k]		1.58[k]		3.02[k]	
	α: 0.3		α: 0.8		α: 0.4		α: 0.9	
62	nd		nd		(78 ± 9)	3	(73 ± 6)	4
	α: nd		α: nd		α: −0.59 ± 0.07		α: −0.88 ± 0.06	
63	nd		nd		(2000 ± 400)	3	(19.1 ± 0.3)	2
	α: nd		α: nd		α: −0.56 ± 0.02		α: −0.54 ± 0.10	

DOI: 10.1021/acs.jmedchem.6b00120
J. Med. Chem. XXXX, XXX, XXX−XXX

Table 2. continued

[a]Functional [^{35}S]GTPγS binding assays with membrane preparations of Sf9 cells expressing the hH_3R + $G\alpha_{i2}$ + $G\beta_1\gamma_2$ or the hH_4R + $G\alpha_{i2}$ + $G\beta_1\gamma_2$ or the hH_2R-$Gs_{\alpha s}$ fusion protein. [b]Steady-state GTPase activity in Sf9 cell membranes expressing the hH_1R + RGS4. [c]Displacement of [^{3}H]**64** (5 nM), [^{3}H]**65** (10 nM), [^{3}H]**66** (3 nM), or [^{3}H]**60** (5 nM) from Sf9 insect cell membranes expressing the hH_1R + RGS4, hH_2R-$Gs\alpha_S$ fusion protein, hH_3R + $G\alpha_{i2}$ + $G\beta_1\gamma_2$ or the hH_4R + $G\alpha_{i2}$ + $G\beta_1\gamma_2$. [d]Reaction mixtures contained ligands at a concentration from 1 nM to 1 mM as appropriate to generate saturated concentration−response curves. N gives the number of independent experiments performed in duplicate each. Agonistic potencies are expressed as EC_{50} values. na = not applicable. EC_{50} values could not be determined due to lacking or extremely low agonist activity. nd = not determined. Intrinsic activities (α) refer to the maximal response induced by the standard agonist histamine (α = 1.0). Compounds identified to be inactive as agonists (α < 0.1 or negative values, respectively, when determined in the agonist mode) were investigated in the antagonist mode. The corresponding K_B values of neutral antagonists and inverse agonists were determined from the concentration-dependent inhibition of the histamine-induced response. The α values of neutral antagonists and inverse agonists were determined at a concentration of 10 μM. [e]K_i values were determined instead of K_B values: **16**, **17**, **31**−**34**, **37**, **41**, **42**, **46**, **47**, >10000 nM; **35**, 8750 ± 290 nM; **36**, 8350 ± 900 nM; **38**, 9350 ± 210 nM. [f]Ref 61. [g]Ref 62. [h]Ref 37 GTPase assays on Sf9 cell membranes. [i]α = 0 (neutral antagonism): the measured values were in the range between +0.15 and −0.15 and not different from 0 when the SEM values were taken into consideration. [j]Ref 39. [k]Ref 60.

Table 3. Pharmacological Data of the Enantioseparated Cyanoguanidines 31a,b, 32a,b, 39a,b, and 40a,b at the hH_xR Subtypes, Determined in the [^{35}S]GTPγS[a] or the GTPase Assay[b] (EC_{50} and K_B Values) and in Radioligand Binding Experiments (K_i Values)[c,d]

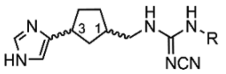

31a,b, 32a,b: R = CH_3
39a,b, 40a,b: R = $(CH_2)_2SPh$

		hH_1R		hH_2R		hH_3R		hH_4R	
no.	configuration	[K_i], EC_{50} or (K_B), nM	N	[K_i], EC_{50} or (K_B), nM	N	[K_i], EC_{50} or (K_B), nM	N	[K_i], EC_{50} or (K_B), nM	N
31a	(1*R*,3*R*)	[>10000]	2	[>10000]	2	[5680 ± 316]	2	[870 ± 57]	4
		na	2	(>10000)	2	9200 ± 400	2	1100 ± 99	3
		α: 0[e]		α: 0[e]		α: 0.29 ± 0.07		α: 0.66 ± 0.19	
31b	(1*S*,3*S*)	[>10000]	2	[>10000]	2	[958 ± 29]	2	[98 ± 11]	4
		na	2	(>10000)	2	994 ± 71	2	100 ± 16	3
		α: 0[e]		α: 0[e]		α: 0.59 ± 0.04		α: 0.66 ± 0.14	
32a	(1*S*,3*R*)	[>10000]	2	[>10000]	2	[9500 ± 1300]	2	[3500 ± 75]	4
		na	2	(>10000)	2	(2812 ± 9)	2	2675 ± 272	3
		α: 0[e]		α: 0[e]		α: −0.14 ± 0.07		α: 0.32 ± 0.06	
32b	(1*R*,3*S*)	[>10000]	2	[>10000]	2	[480 ± 100]	2	[120 ± 7]	4
		na	2	(>10000)	2	212 ± 33	2	119 ± 20	3
		α: 0[e]		α: 0[e]		α: 0.61 ± 0.07		α: 0.86 ± 0.02	
39a	(1*S*,3*S*)	[6520 ± 570]	2	[10300 ± 500]	2	[2130 ± 17]	3	[22 ± 3]	5
		na	2	(>10000)	2	(1150 ± 112)	3	11 ± 2	3
		α: 0[e]		α: 0[e]		α: 0[e]		α: 0.75 ± 0.04[f]	
39b	(1*R*,3*R*)	[7910 ± 710]	2	[9820 ± 90]	2	[590 ± 36]	3	[1050 ± 120]	5
		na	2	(>10000)	2	(143 ± 12)	2	(7700 ± 400)	2
		α: 0[e]		α: 0[e]		α: −0.21 ± 0.04		α: 0[e]	
40a	(1*S*,3*R*)	[6780 ± 300]	2	[7360 ± 480]	2	[745 ± 8]	3	[290 ± 30]	5
		na	2	(>10000)	2	(528 ± 50)	2	549 ± 8	3
		α: 0[e]		α: 0[e]		α: −0.34 ± 0.04		α: 0.54 ± 0.09	
40b	(1*R*,3*S*)	[3050 ± 260]	2	[7250 ± 140]	2	[870 ± 22]	3	[180 ± 22]	5
		na	2	(>10000)	2	(718 ± 12)	2	293 ± 32	3
		α: 0[e]		α: 0[e]		α: −0.21 ± 0.03		α: 0.39 ± 0.01	

[a]Data were analyzed for best fit to one site (monophasic) competition curves. *N* gives the number of independent experiments performed in duplicate; na = not applicable, EC_{50} values could not be determined due to lacking or extremely low agonist activity. Functional [^{35}S]GTPγS binding assays with membrane preparations of Sf9 cells expressing the hH_3R + $G\alpha_{i2}$ + $G\beta_1\gamma_2$ or the hH_4R + $G\alpha_{i2}$ + $G\beta_1\gamma_2$ or the hH_2R-$Gs_{\alpha s}$ fusion protein. [b]Steady-state GTPase activity in Sf9 cell membranes expressing the hH_1R + RGS4. [c]Displacement of [^{3}H]**64** (5 nM), [^{3}H]**65** (10 nM), [^{3}H]**66** (3 nM), or [^{3}H]**60** (5 nM) from Sf9 insect cell membranes expressing the hH_1R + RGS4, hH_2R-$Gs\alpha_S$ fusion protein, hH_3R + $G\alpha_{i2}$ + $G\beta_1\gamma_2$ or the hH_4R + $G\alpha_{i2}$ + $G\beta_1\gamma_2$. [d]Reaction mixtures contained ligands at a concentration from 1 nM to 1 mM as appropriate to generate saturated concentration−response curves. N gives the number of independent experiments performed in duplicate each. Agonistic potencies are expressed as EC_{50} values. na = not applicable. EC_{50} values could not be determined due to lacking or extremely low agonist activity. nd = not determined. Intrinsic activities (α) refer to the maximal response induced by the standard agonist histamine (α = 1.0). Compounds identified to be inactive as agonists (α < 0.1 or negative values, respectively, when determined in the agonist mode) were investigated in the antagonist mode. The corresponding K_B values of neutral antagonists and inverse agonists were determined from the concentration-dependent inhibition of the histamine-induced response. The α values of neutral antagonists and inverse agonists were determined at a concentration of 10 μM. [e]α = 0 (neutral antagonism): the measured values were in the range between +0.15 and −0.15 and not different from 0 when the SEM values were taken into consideration. [f]The intrinsic activities of the eutomer **39a** (α = 0.75) and the racemate **39** (α = 0.90) were not significantly different from each other (*p*-value: 0.2).

DOI: 10.1021/acs.jmedchem.6b00120
J. Med. Chem. XXXX, XXX, XXX−XXX

activity was observed at the H_1R and the H_2R. All investigated racemates revealed very weak H_2R antagonism with K_B values >10 μM. At the H_1R, the compounds were weak antagonists (**31**−**34** and **39**−**42**, **46**) or inverse agonists (**35**−**38**, **47**), respectively. Except for **39** (K_B = 6 μM) and **40** (K_B = 3.8 μM) the K_B values were in the high micromolar range.

The racemates of the phenylsulfanylethyl substituted cyanoguanidines **39** and **40** turned out to be the most promising candidates for more detailed investigation. Therefore, the enantiomers were prepared as outlined above. In addition, for reasons of comparison with the tetrahydrofuran series, the methyl-substituted cyanoguanidines **31** and **32** were considered as well.

Functional and Binding Data of the Separated Enantiomers at hH_xR Subtypes. The enantiomerically pure compounds **31a,b**, **32a,b**, **39a,b**, and **40a,b** were investigated under the same conditions as the racemates (data cf. Table 3). The results for the enantiomers of **31** and **32** were comparable to the data reported for the tetrahydrofuran **4** and analogues. The enantiomers *trans*-(−)-**31** (**31a**) and *cis*-(−)-**32** (**32a**) were both weak H_4R partial agonists with EC_{50} values >1 μM. The eutomers, *trans*-(+)-**31** (**31b**) and *cis*-(+)-**32** (**32b**), were moderately potent H_4R agonists with EC_{50} values around 100 nM. Compared to the H_4R, the potencies and efficacies were lower at the H_3R: **32a** was an inverse agonist, whereas the other three isomers were weak partial agonists with α values in the range 0.3−0.6. Similar to the stereodiscrimination at the H_4R, **31b** and **32b** were by a factor of 10 more potent than their optical antipodes at the H_3R. As for the racemates, no relevant activities were detected at the H_1R and the H_2R. The most potent and selective H_4R agonist among these four stereoisomers was the carba analogue of **4**, *trans*-(+)-(1*S*,3*S*)-**31** (**31b**) (**4**, EC_{50} reported, 78 nM, α = 0.99;[42] **31b**, EC_{50} = 100 nM, α = 0.71). Obviously, the exchange of the oxygen atom in **4** by a carbon atom does not markedly affect the pharmacological activity. The correlation between the absolute configuration of the four stereoisomers and their pharmacological properties at the H_3R and the H_4R is in agreement with the data for the structurally related tetrahydrofuran derivatives reported by Hashimoto et al.[42]

The evaluation of the separated enantiomeric pairs **39** and **40** revealed **39a** as a potent and selective H_4R agonist: **39a** activated the H_4R with an EC_{50} value of 11 nM and an intrinsic activity of 0.75 in the [^{35}S]GTPγS binding assay (Figure 6. By contrast, at the H_3R **39a** was a weak antagonist (K_B = 1150 nM), corresponding to a more than 100-fold selectivity for the H_4R. The activities at the other two histamine receptor subtypes were negligible. Surprisingly, the investigation of the optical antipode of **39a**, compound **39b**, revealed just the opposite profile: **39b** was a weak neutral antagonist at the H_4R (K_B = 7700 nM) but almost 10 times more active as an antagonist (inverse agonist) at the H_3R (K_B = 143 nM, α = −0.21) compared to **39a**. Both *cis*-configured enantiomers, **40a** and **40b**, were moderately potent H_4R partial agonists with EC_{50} values in the three-digit nanomolar range and H_3R inverse agonists with K_B values of 528 and 718 nM, respectively. At the H_2R and H_1R, these compounds were devoid of agonistic activity but showed weak antagonism in the micromolar range.

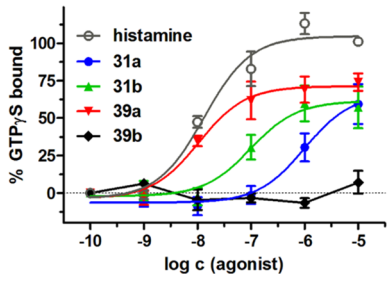

Figure 6. [^{35}S]GTPγS binding at the hH_4R. Functional [^{35}S]GTPγS binding assays were performed with membrane preparations of Sf9 cells expressing the hH_4R + $G\alpha_{i2}$ + $G\beta_1\gamma_2$. Data were analyzed by nonlinear regression and were best fit to sigmoidal concentration−response curves. Data points shown are the means of three independent experiments performed in duplicate each.

Comparing the whole set of eight enantioseparated imidazolylcyclopentylcyanoguanidines, highest H_4R agonistic potency always resided in the stereoisomers with *S*-configuration in position 3. Obviously, the configuration at position 1 is less important, although (1*S*)-configuration is preferred, in particular, in the case of compounds bearing substituents larger than methyl at the cyanoguanidine moiety. Regarding the H_3R, there was no clear correlation between configuration and potency. Nevertheless, as compound **39b**, the most potent H_3R ligand in this series is *trans*-(1*R*,3*R*)-configured, the optimal stereochemical requirements for H_3R and H_4R affinity seem to be converse. Hence, both highest H_4R agonistic potency and H_4R subtype selectivity resided in *trans*-(1*S*,3*S*)-configured compounds. These results are in principle in agreement with the spatial orientation of the substituents at the tetrahydrofuran ring in **4**. Moreover, in accordance with the imidazolylalkylcyanoguanidine series, a phenylsulfanylethyl substituent and a chain length of four carbon atoms between imidazole and cyanoguanidine moiety confer high H_4R potency and selectivity.

Especially for the H_4R, differences between pharmacological data from various studies are reported,[28,35] and even the quality of action may differ,[35] depending on test system and read-out. For validation, the racemates **39** and **40** as well as the corresponding enantiomers **39a,b** and **40a,b** were also investigated in steady-state GTPase assays on hH_4R and hH_3R (data not shown). The determined potencies and efficacies were comparable to those from the [^{35}S]GTPγS binding assays. The [^{35}S]GTPγS binding induced by histamine or **39a** was inhibited by standard H_4R antagonists in a concentration-dependent manner and gave comparable results, for example: **62**, K_B 73 ± 6 nM vs histamine and 100 ± 14 nM vs **39a**; **63**, K_B 19 ± 0.3 nM vs histamine and 29 ± 2 nM vs **39a**. The K_B values determined for **61** (19 ± 6 nM), **62**, and **63** against **39a** were in the same range as K_i values from binding studies reported by Lim et al. (**61**, 16 nM; **62**, 125 nM; **63**, 13 nM)[38] and Wifling et al. (**62**, 178 nM; **63**, 69 nM).[63] These results confirm **39a** to act as a hH_4R agonist in the [^{35}S]GTPγS binding assay and to compete with the H_4R antagonists for the same binding site. Furthermore, **39a** displaced [^{3}H]histamine from the hH_4R, providing additional evidence of binding to the same site.

The H_4R agonist potency of **39a** (Table 3) was higher than that of **1**, **58**, and **59** but lower than in case of the acylguanidine **60** (Table 2). The selectivity of **39a** for the H_4R over the H_3R was slightly lower than that of **58**. With respect to the application of such compounds as molecular tools, in addition to binding affinities, the quality of action has to be considered. In contrast to the reference H_4R agonists **58**−**60**, compound

DOI: 10.1021/acs.jmedchem.6b00120
J. Med. Chem. XXXX, XXX, XXX−XXX

39a was devoid of agonist activity at H_1, H_2, and H_3 receptors like **1**.

H_4R Agonism in the Reporter Gene Assay. Selected enantiomers were investigated in a luciferase reporter gene assay on HEK-293 cells stably expressing the human or the mouse H_4R (Figure 7).

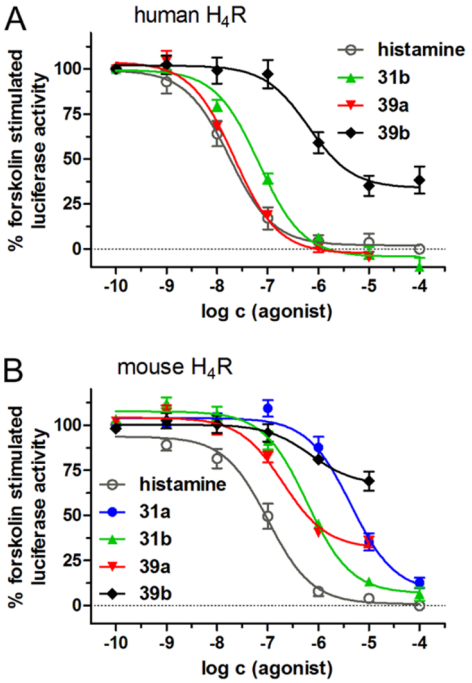

Figure 7. Inhibition of forskolin stimulated luciferase activity by H_4R agonists. (A) HEK293-SF-hH_4R-His_6-CRE-Luc cells expressing the hH_4R; forskolin concentration, 400 nM. (B) HEK293-SF-mH_4R-His_6-CRE-Luc cells expressing the mH_4R; forskolin concentration, 1 μM. Reaction mixtures contained ligands at concentrations from 1 nM to 100 μM as appropriate to generate saturated concentration−response curves. Data represent mean values ± SEM of five (histamine at the hH_4R) or, in all other cases, four independent experiments performed in triplicate. The intrinsic activity (α) of histamine was set to 1.0 and maximal responses α of test compounds were referred to this value. EC_{50} values at the hH_4R: histamine, 13 ± 4 nM, α = 1.0; **31b**, 63 ± 4 nM, α = 1.0; **39a**, 25 ± 2 nM, α = 1.0; **39b**, 500 ± 150 nM, α = 0.6. EC_{50} values at the mH_4R: histamine, 94 ± 29 nM, α = 1.0; **31a**, 3631 ± 1160 nM, α = 0.96; **31b**, 538 ± 33 nM, α = 0.96; **39a**, 166 ± 20 nM, α = 0.67; **39b**, 589 ± 162 nM, α = 0.29.

The data obtained for **31b** and **39a** at the hH_4R were comparable to the results of the [^{35}S]GTPγS and radioligand binding assays. Both compounds were full hH_4R agonists with EC_{50} values in the low nanomolar range. Interestingly, **39b**, which was a weak neutral antagonist in the [^{35}S]GTPγS assay, showed partial agonism with an EC_{50} value of 500 nM in the luciferase assay. This apparent discrepancy, depending on either a proximal (G-protein activation in Sf9 cell membranes) or a distal readout (reporter gene assay), can be explained by signal amplification downstream from G-protein activation in the cellular assay.[33] Regardless of this, the high H_4R agonistic potency of the eutomer **39a** and the stereodiscrimination (cf. **39b**) by the human receptor was confirmed in the cell based luciferase reporter gene assay. Species-dependent discrepancies regarding potencies and receptor selectivities are characteristic of numerous pharmacological tools for the H_4R,[29,31,36] and comparable potencies at the human and the murine H_4R, as described for several oxime-type agonists,[64] are desired with respect to translational animal models. Therefore, the separated enantiomers were also investigated at the mouse H_4R in the luciferase assay (Figure 7B and Supporting Information). As becomes obvious from Figure 7, lower potency and intrinsic activity as well as lower stereodiscrimination was characteristic of the enantiomers at the mouse compared to the human H_4R.

H_xR Subtype Affinities of the Separated Enantiomers. Binding data (K_i values) of the enantiomers of **31**, **32**, **39**, and **40** were determined at the four hHR subtypes (Table 3, Figure 8). Competition binding studies on the hH_4R were performed

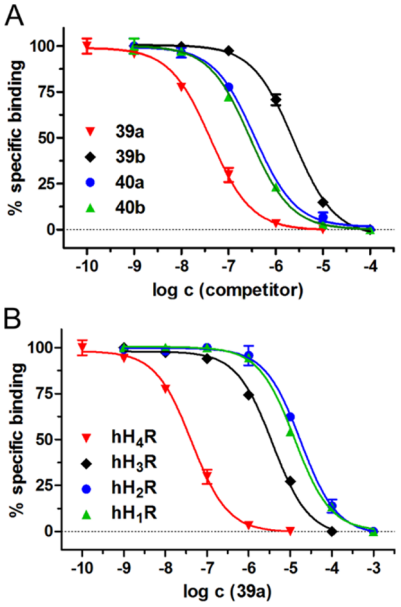

Figure 8. Representative radioligand binding experiments: (A) displacement of [^{3}H]**60** (5 nM) from Sf9 insect cell membranes expressing the hH_4R + Gα_{i2} + G$\beta_1\gamma_2$. (B) Displacement of [^{3}H]**64** (5 nM; K_D 4.49 nM), [^{3}H]**65** (10 nM; K_D 32 nM), [^{3}H]**66** (3 nM; K_D 8.4 nM) and [^{3}H]**60** (5 nM; K_D 12.6 nM) from Sf9 insect cell membranes expressing the hH_1R + RGS4, hH_2R-Gsα_S fusion protein, hH_3R + Gα_{i2} + G$\beta_1\gamma_2$ or the hH_4R + Gα_{i2} + G$\beta_1\gamma_2$. Data were analyzed for best fit to one site (monophasic) competition curves.

with two different radioligands, which gave comparable results: the standard compound [^{3}H]histamine and [^{3}H]**60**,[59] an acylguanidine developed in our laboratory. All evaluated compounds displaced [^{3}H]**64** ([^{3}H]mepyramine) from the hH_1R, [^{3}H]**65** ([^{3}H]tiotidine) from the hH_2R, [^{3}H]**66** ([^{3}H]N$^{\alpha}$-methylhistamine) from the hH_3R, and [^{3}H]**60** or [^{3}H]histamine from the hH_4R, giving monophasic competition binding curves (Figure 8).

Although for most compounds the K_i values from radioligand binding experiments were slightly higher than the EC_{50} values determined in the [^{35}S]GTPγS assay, in general, the binding data and the rank order of the compounds were in agreement with the potencies evaluated in the functional assays. As expected, **39a** bound with the highest affinity to the hH_4R (K_i = 22 nM) and showed a remarkably lower affinity for the hH_3R (K_i = 2130 nM). At the hH_2R and the hH_1R, all compounds displayed low affinity. Overall, the determined K_i values confirmed **39a** to be a highly affine and selective ligand for the hH_4R.

Binding Mode of 39a and 39b at the hH_4R. Molecular dynamic simulations revealed a stable binding mode of **39a** in

DOI: 10.1021/acs.jmedchem.6b00120
J. Med. Chem. XXXX, XXX, XXX−XXX

the hH_4R−G$\alpha i2\beta\gamma$ complex active state. The central cyanoguanidine moiety interacted electrostatically with the highly conserved $Asp^{3.32}$ (Figure 9A). The positively charged

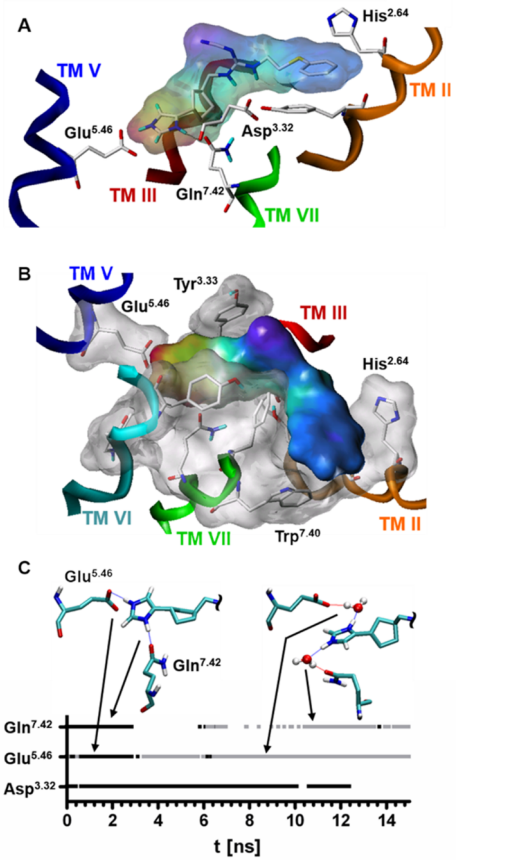

Figure 9. Binding mode of **39a** in the active state model of the hH_4R−G$\alpha i2\beta\gamma$ complex, obtained by molecular dynamic simulations. (A) Orientation of **39a** in the orthosteric binding pocket, caused by the interactions of the imidazole moiety with $Glu^{5.46}$ and the cyanoguanidine moiety with $Asp^{3.32}$. (B) Contact surface between **39a** and the amino acids of the orthosteric binding pocket. (C) Time domains of direct H-bond interactions (black) and water-mediated H-bond interactions (gray) between **39a** and the hH_4R.

imidazole moiety was embedded in a pocket between transmembrane domain (TM) III, TM VI, and TM VII, formed by $Tyr^{3.33}$, $Trp^{6.48}$, and $Tyr^{6.51}$. Furthermore, the imidazole moiety was found to interact with $Glu^{5.46}$ (Figure 9B). Within the first 3 ns of the simulation, direct interactions between the imidazole moiety and $Glu^{5.46}$ and $Gln^{7.42}$ were observed (Figure 9A). After 3 ns, the imidazole moiety changed its orientation. The interactions between the imidazole and $Glu^{5.46}$ and $Gln^{7.42}$ were then mediated by two water molecules (Figure 9C). This conformation remained stable for the remaining 12 ns of MD simulation. Taking into account the direct and the water-mediated hydrogen bond interactions between **39a** and the hH_4R, **39a** is stabilized in the binding pocket by a total of four to five H-bonds. Additionally, the molecular dynamic simulations revealed an aromatic interaction of the phenyl moiety of **39a** with the aromatic amino acids $Tyr^{2.61}$, $His^{2.64}$, $Phe^{7.39}$, and $Trp^{7.40}$.

Because **39a** was a hH_4R partial agonist in the [^{35}S]GTPγS assay (Table 3), molecular dynamic simulations of **39a** at the inactive hH_4R were performed, too. A mean of ∼4.5 direct hydrogen bond interactions between **39a** and the inactive hH_4R was determined. In accordance with **39a**, in the active state hH_4R−G$\alpha i2\beta\gamma$ complex, stable hydrogen bond interactions between the cyanoguanidine moiety and $Asp^{3.32}$ and between the positively charged imidazole moiety with $Glu^{5.46}$ were observed. Additionally, the imidazole moiety was stabilized by a hydrogen bond with $Ser^{6.52}$ (Figure 10A, left) or, alternatively,

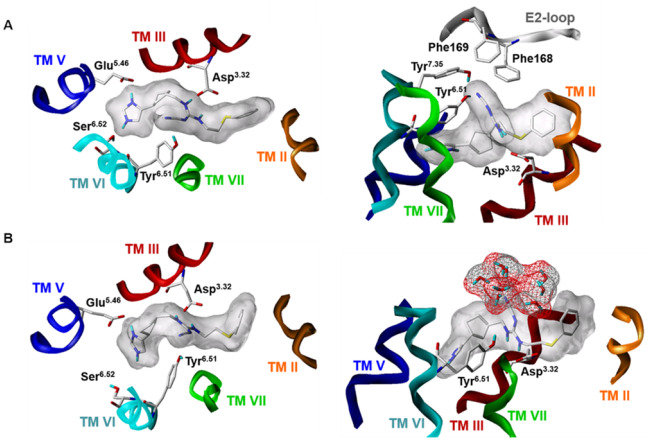

Figure 10. Binding mode of **39a** and **39b** in the inactive state model of the hH_4R, obtained by molecular dynamic simulations. (A) Orientation of **39a** in the orthosteric binding pocket, forming H-bond interactions with $Asp^{3.32}$, $Glu^{5.46}$, and $Ser^{6.52}$ (left, top view; right, side view). (B) Orientation of **39b** in the orthosteric binding pocket, forming H-bond interactions with $Asp^{3.32}$ and $Glu^{5.46}$ (left, top view; right, side view).

with $Thr^{6.55}$. Furthermore, $Tyr^{6.51}$ (Figure 10A, right) interacted with the nitrile group of the cyanoguanidine moiety. In contrast to **39a** bound to the active state hH_4R−G$\alpha i2\beta\gamma$ complex, an interaction between the ligand and $Gln^{7.42}$ was not observed. The phenyl moiety was embedded in an aromatic pocket comprising $Tyr^{2.61}$, $His^{2.64}$, $Trp^{3.28}$, and $Phe^{7.39}$.

Molecular dynamic simulations of the neutral antagonist **39b** in the binding pocket of the inactive hH_4R showed a strong interaction of the cyanoguanidine moiety with $Asp^{3.32}$ and of the positively charged imidazole moiety with $Glu^{5.46}$. Compared to **39a**, only a mean number of approximately three direct hydrogen bond interactions between ligand and receptor was observed during the MD simulation, which may explain the lower hH_4R affinity of **39b** compared to **39a**. An interaction between the imidazole moiety and $Ser^{6.52}$ or $Thr^{6.55}$ was not detected (Figure 10B, left). Thus, a second stabilizing hydrogen bond between the imidazole moiety and the hH_4R, as observed for **39a**, was not present. Furthermore, an interaction between $Tyr^{6.51}$ and the cyano group was not observed (Figure 10B, right). In contrast to **39a**, the cyano group of **39b** was not surrounded by amino acids of the hH_4R but solvated by extracellular water (Figure 10B right). Thus, compared to **39a**, there were less interactions with the receptor. Comparable to **39a** at the inactive hH_4R, the phenyl moiety of **39b** was surrounded by aromatic amino acids ($Tyr^{2.61}$, $His^{2.64}$, $Trp^{3.28}$, $Phe^{7.39}$) and showed a similar flexibility in its pocket.

The imidazole moieties of the enantiomers **39a** and **39b** are embedded in slightly different orientations in the binding pocket of hH_4R, resulting in a higher number of hydrogen bonds in case of **39a**. This is in accordance with the higher hH_4R affinity of **39a** compared to **39b**.

DOI: 10.1021/acs.jmedchem.6b00120
J. Med. Chem. XXXX, XXX, XXX−XXX

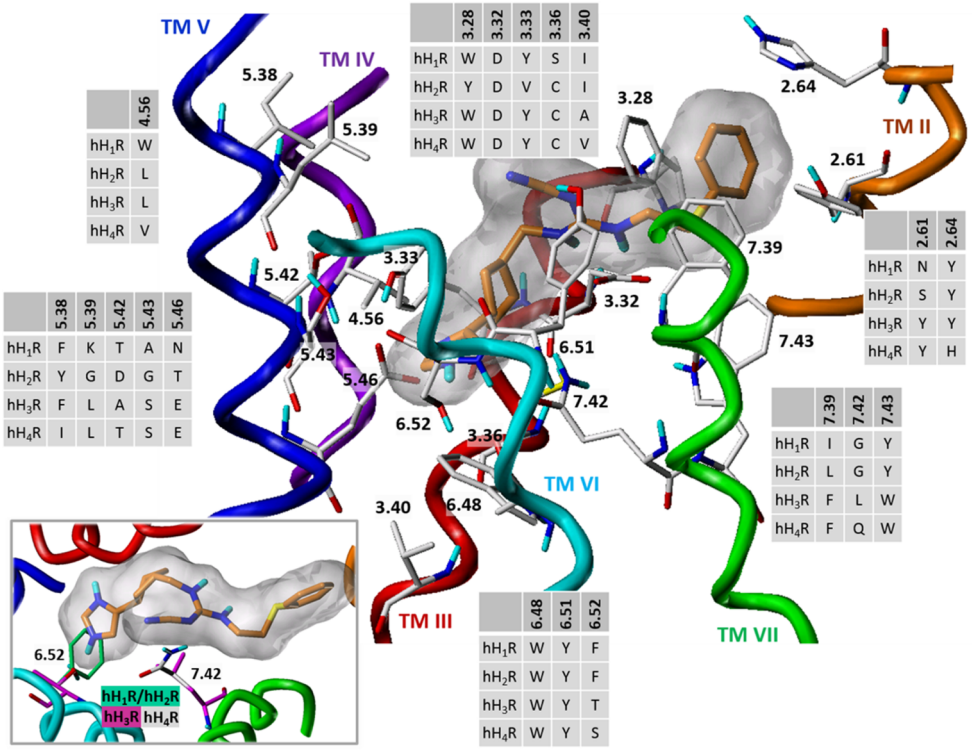

	4.56
hH_1R	W
hH_2R	L
hH_3R	L
hH_4R	V

	3.28	3.32	3.33	3.36	3.40
hH_1R	W	D	Y	S	I
hH_2R	Y	D	V	C	I
hH_3R	W	D	Y	C	A
hH_4R	W	D	Y	C	V

	2.61	2.64
hH_1R	N	Y
hH_2R	S	Y
hH_3R	Y	Y
hH_4R	Y	H

	5.38	5.39	5.42	5.43	5.46
hH_1R	F	K	T	A	N
hH_2R	Y	G	D	G	T
hH_3R	F	L	A	S	E
hH_4R	I	L	T	S	E

	7.39	7.42	7.43
hH_1R	I	G	Y
hH_2R	L	G	Y
hH_3R	F	L	W
hH_4R	F	Q	W

	6.48	6.51	6.52
hH_1R	W	Y	F
hH_2R	W	Y	F
hH_3R	W	Y	T
hH_4R	W	Y	S

Figure 11. Comparison of the binding sites of the four human histamine receptor subtypes. Center: Section of the hH_4R with bound compound **39a**. Tables: Key amino acids in the respective binding pockets of the individual receptor subtypes. Inset: Compared to the orientation of **39a** in the hH_4R binding site (gray), the amino acids present at positions 6.52 and 7.42 of the hH_1R, the hH_2R, and the hH_3R (color-coded and superimposed with the hH_4R model for visualization) disfavor the binding of **39a**.

The exchange of the CH_3 group in **31b** by a $(CH_2)_2SPh$ moiety (**39a**) resulted in an increase in hH_4R affinity and agonist potency (Table 3). As suggested by the molecular dynamic studies, the phenyl ring of **39a** is embedded in an aromatic pocket of the hH_4R (Figure 11), formed by $Tyr^{2.61}$, $His^{2.64}$, $Trp^{3.28}$, and $Phe^{7.39}$. These interactions are not present in case of the methyl substituted analogue **31b**.

The affinity of **39a** is more than 100-fold higher to the hH_4R than to hH_1R, hH_2R, or hH_3R (Table 3). Comparing the binding pocket of the four human histamine receptor subtypes (Figure 11), only $Asp^{3.32}$, $Trp^{6.48}$, and $Tyr^{6.51}$ are conserved. Regarding the amino acids specified in Figure 11, the hH_4R shares only 20% and 30% with the hH_1R and the hH_2R, respectively. In contrast, about 63% of the respective amino acids are identical in hH_3R and hH_4R. There is a difference between the hH_3R and the hH_4R regarding the amino acids at positions 6.52 and 7.42, which are in contact with the imidazole ring and the cyanoguanidine group of **39a** in the case of the hH_4R (Figure 11). Interactions of $Ser^{6.52}$ and $Gln^{7.42}$ via hydrogen bonds with **39a** were detected in the MD simulations. The lower affinity of **39a** to the hH_3R may be attributed, at least in part, to the presence of $Leu^{7.42}$ instead of $Gln^{7.42}$, which precludes this interaction. Moreover, it may be speculated that the methyl group of $Thr^{6.52}$, which is present in the hH_3R instead of $Ser^{6.52}$ in the hH_4R, disfavors the orientation of the ligand in the H_3R binding pocket.

The very low affinity of **39a** at the hH_1R and the hH_2R compared to the hH_4R may be attributed to $Phe^{6.52}$, which prevents the formation of a hydrogen bond and causes a collision with the imidazole ring of **39a** (Figure 11, inset). In the case of **39b**, a hydrogen bond between the imidazole moiety and $Ser^{6.52}$ of the hH_4R was not observed in the MD simulation. Furthermore, compared to **39a**, the imidazole moiety of **39b** was more distant from TM VI. Therefore, presumably, there is no collision between $Phe^{6.52}$ and the imidazole ring at the hH_1R and the hH_2R. This may explain the lower histamine receptor subtype selectivity of **39b** compared to its optical antipode **39a**. The low homology of the binding site of the hH_4R compared to those of the hH_1R and the hH_2R (Figure 11) suggests that amino acids other than those in positions 6.52 and 7.42 also contribute to hH_4R selectivity.

CONCLUSIONS

Conformationally constrained analogues of the imidazolylbutylcyanoguanidine **1**, a potent hH_4R agonist with some selectivity over the H_3R, were obtained by incorporation of a cyclopentane-1,3-diyl moiety and identification of the most active enantiomer according to a step-by-step approach. At both the H_4R and the H_3R, the pharmacological properties were strongly dependent on the stereochemistry of the cyclopentane-1,3-diyl moiety. At the H_4R, a preference for *trans* configured compounds was observed except for the methyl-substituted cyanoguanidines. At the H_3R, *cis* configuration was preferred in most cases. None of the investigated compounds showed agonistic activity at the H_1R and H_2R. Phenylsulfanylethyl-substituted cyanoguanidines turned out to be superior to compounds with other substituents including methyl as in case of the carba analogues of **4**, that is the *trans*- and *cis*-configured compounds **31** and **32**, respectively. Starting from a set of racemic compounds, the most promising H_4R agonists were selected for chiral separation by HPLC. In addition, an enzyme assisted stereoselective synthesis enabled the assignment of the absolute configurations. Highest receptor subtype selectivity and H_4R agonist potency, determined in a

DOI: 10.1021/acs.jmedchem.6b00120
J. Med. Chem. XXXX, XXX, XXX−XXX

proximal functional assay ([^{35}S]GTPγS binding), resided in the *trans*-(1*S*,3*S*)-configured compound **39a**. By contrast, the optical antipode **39b** was an H_4R antagonist under the same conditions. Obviously, *trans*-(1*S*,3*S*)-**39a** is capable of stabilizing the H_4R active state, whereas *trans*-(1*R*,3*R*)-**39b** prefers the inactive state, as supported by MD simulations. Thus, the conformationally constrained ligand **39a** may be useful as a pharmacological tool, providing stereochemical information for the refinement of models of the binding mode of imidazolylalkyl-substituted cyanoguanidine-type H_4R agonists.

EXPERIMENTAL SECTION

Chemistry: General Conditions. Commercial reagents and chemicals were purchased from Acros Organics (Geel, Belgium), IRIS Biotech GmbH (Marktredwitz, Germany), Alfa Aesar GmbH & Co. KG (Karlsruhe, Germany), Merck KGaA (Darmstadt, Germany), Sigma-Aldrich Chemie GmbH (Munich, Germany), and TCI Europe (Zwijndrecht, Belgium) and used without further purification. Deuterated solvents for NMR spectroscopy were from Deutero GmbH (Kastellaun, Germany). All solvents were of analytical grade or distilled prior to use. Millipore water was used throughout for the preparation of buffers and HPLC eluents. If moisture-free conditions were required, reactions were performed in dried glassware under inert atmosphere (argon or nitrogen). Anhydrous DMF was purchased from Sigma-Aldrich Chemie GmbH and stored over 3 Å molecular sieves. Cholesterol esterase from porcine pancreas (EC 3.1.1.13) was from Sigma-Aldrich Chemie GmbH (Munich, Germany). Optical rotations were measured on a PerkinElmer 141 polarimeter in the specified solvent. Concentrations are indicated in [g/100 mL]. Flash chromatography was performed in glass columns on silica gel (Merck silica gel 60, 40−63 μm). Automated flash chromatography was performed on a Varian IntelliFlash 310 using prepacked Varian Superflash columns (Varian, Darmstadt, Germany). Reactions were monitored by TLC on aluminum plates coated with silica gel (Merck silica gel 60 F_{254}, thickness 0.2 mm). The compounds were detected by UV light (254 nm), a 0.3% solution of ninhydrine in *n*-butanol (amines), and a 1.0% solution of Fast Blue B salt (imidazole containing compounds) in EtOH/H_2O = 30/70 (v/v) or iodine staining. All melting points are uncorrected and were measured on a Büchi 530 (Büchi GmbH, Essen, Germany) apparatus. Lyophilization was done with a Christ alpha 2-4 LD equipped with a vacuubrand RZ 6 rotary vane vacuum pump. Microwave assisted reactions were performed on an Initiator 2.0 synthesizer (Biotage, Uppsala, Sweden). Nuclear magnetic resonance spectra (^{1}H NMR and ^{13}C NMR) were recorded with Bruker Avance 300 (^{1}H, 300.1 MHz; ^{13}C, 75.5 MHz), Avance 400 (^{1}H, 400.1 MHz; ^{13}C, 100.6 MHz) or Bruker Avance 600 (^{1}H, 600.1 MHz; ^{13}C, 150.9 MHz) NMR spectrometers (Bruker BioSpin GmbH, Rheinstetten, Germany). Chemical shifts are given in δ (ppm) relative to external standards. Abbreviations for the multiplicities of the signals: s (singlet), d (doublet), t (triplet), m (multiplet), brs (broad singlet), and combinations thereof. The multiplicity of carbon atoms (^{13}C NMR) was determined by DEPT 135 (distortionless enhancement by polarization transfer): "+" primary and tertiary carbon atom (positive DEPT 135 signal), "−" secondary carbon atom (negative DEPT 135 signal), "C_{quat}" quaternary carbon atom. In certain cases 2D-NMR techniques (COSY, HMQC, HSQC, HMBC, NOESY) were used to assign ^{1}H and ^{13}C chemical shifts. Infrared spectra (IR) were measured on a Bruker Tensor 27 spectrometer equipped with an ATR (attenuated total reflection) unit from Harrick Scientific Products Inc. (Ossinning/NY, US). Mass spectra (MS) were recorded on a Finnigan MAT 95 (EI-MS 70 eV, HR-MS), Finnigan SSQ 710A (CI-MS (NH_3)), and on a Finnigan ThermoQuest TSQ 7000 (ES-MS) spectrometer. The peak-intensity in % relative to the strongest signal is indicated in parentheses. Elemental analysis (C, H, N, Heraeus Elementar Vario EL III) were performed by the Analytical Department of the University Regensburg and are within ±0.4% unless otherwise noted.

Analytical HPLC analysis was performed on a system from Thermo Separation Products (TSP, Egelsbach, Germany) composed of a SN400 controller, a P4000 pump, an AS3000 autosampler, a degasser (Degassex DG-4400, Phenomenex), a Spectra Focus UV−vis detector, and a RP column thermostated at 30 °C ((a) Eurosphere-100 C18, 250 mm × 4.0 mm, 5 μm, Knauer, Berlin, Germany, t_0 = 3.32 min; (b) MN Nucleodur 100−5 C18 ec, 250 mm × 4.0 mm, 5 μm, Macherey Nagel, Düren, Germany, t_0 = 2.68 min; (c) Luna C18-2, 150 mm × 4.6 mm, 4 μm, Phenomenex, Aschaffenburg, Germany, t_0 = 2.88 min) at a flow rate of 0.8 mL/min. UV detection was done at 220 nm. Mixtures of acetonitrile and 0.05% aq TFA were used as mobile phase. Helium degassing was used throughout. Compound purities were calculated as percentage peak area of the analyzed compound by UV detection at 220 nm. HPLC conditions, retention times (t_R), capacity factors (k' = (t_R − t_0)/t_0), and purities of the synthesized compounds are listed in the Supporting Information. Purity of tested compounds was >95% as determined by high-performance liquid chromatography.

Chemistry: Experimental Protocols and Analytical Data. Synthesis of the Cyanoguanidines 31−42, 46, and 47. General Procedure.[37,51] The isourea (1 equiv) and the pertinent amine (1 equiv) in MeCN were heated under microwave irradiation at 150 °C for 15 min. After removal of the solvent in vacuo, the crude product was purified by flash chromatography (DCM/MeOH/32% $NH_{3(aq)}$ 95/4/1 v/v/v).

*(±)-2-Cyano-1-{[trans-3-(1H-imidazol-4-yl)cyclopentyl]methyl}-3-methylguanidine (**31**).* The title compound was prepared from **16** (0.05 g, 0.3 mmol) and **25** (0.053 g, 0.3 mmol) in MeCN (4.5 mL) according to the general procedure. Flash chromatography yielded a yellow solid (0.07 g, 95%); mp 41 °C. ^{1}H NMR (300 MHz, CD_3OD): δ [ppm] = 1.35 (m, 1H, CH_2), 1.68 (m, 1H, CH_2), 1.83 (m, 2H, CH_2), 1.94 (m, 1H, CH_2), 2.08 (m, 1H, CH_2), 2.39 (m, 1H, C*H*), 2.79 (s, 3H, CH_3-N), 3.18 (m, 3H, C*H*-Im + CH_2-N), 6.80 (s, 1H, Im-*H*-5), 7.60 (s, 1H, Im-*H*-2). ^{13}C NMR (75 MHz, CD_3OD): δ [ppm] = 28.74 (+, CH_3), 30.96 (−, CH_2), 33.86 (−, CH_2), 37.84 (−, CH_2), 37.71 (+, CH), 39.68 (+, CH), 47.71 (−, CH_2-N), 116.71 (+, Im-C-5), 120.28 (C_{quat}, C≡N), 134.98 (+, Im-C-2), 141.94 (C_{quat}, Im-C-4), 162.05 (C_{quat}, C═N). HRMS (EI-MS) calcd for $C_{12}H_{18}N_6$ [$M^{+\bullet}$] 246.1593; found 246.1587. IR (cm^{-1}) = 3289 (N-H), 3142, 2940, 2864 (C-H), 2163 (C≡N), 1582 (C═N), 1368. Anal. ($C_{12}H_{18}N_6 \cdot 0.5H_2O \cdot CH_3OH$) C, H, N, $C_{12}H_{18}N_6$ (246.31).

*(±)-2-Cyano-1-{[cis-3-(1H-imidazol-4-yl)cyclopentyl]methyl}-3-methylguanidine (**32**).* The title compound was prepared from **17** (0.05 g, 0.3 mmol) and **25** (0.053 g, 0.3 mmol) in MeCN (4.5 mL) according to the general procedure. Flash chromatography yielded a yellow solid (0.065 g, 82%); mp 61−63 °C. ^{1}H NMR (300 MHz, CD_3OD): δ [ppm] = 1.33 (m, 1H, CH_2), 1.50 (m, 1H, CH_2), 1.71 (m, 1H, CH_2), 1.85 (m, 1H, CH_2), 2.03 (m, 1H, CH_2), 2.19 (m, 1H, CH_2), 2.33 (m, 1H, C*H*), 2.79 (s, 3H, CH_3-N), 3.09 (m, 1H, C*H*-Im), 3.18 (m, 2H, CH_2-N), 6.79 (s, 1H, Im-*H*-5), 7.57 (s, 1H, Im-*H*-2). ^{13}C NMR (75 MHz, CD_3OD): δ [ppm] = 28.73 (+, CH_3), 30.07 (−, CH_2), 32.93 (−, CH_2), 38.78 (−, CH_2), 39.01 (+, CH), 40.71 (+, CH), 47.82 (−, CH_2−N), 116.75 (+, Im-C-5), 120.29 (C_{quat}, C≡N), 135.87 (+, Im-C-2), 141.94 (C_{quat}, Im-C-4), 162.02 (C_{quat}, C═N). HRMS (EI-MS) calcd for $C_{12}H_{18}N_6$ [$M^{+\bullet}$] 246.1593; found 246.1593. IR (cm^{-1}) = 3258 (N-H), 3149, 2930, 2869 (C-H), 2160 (C≡N), 1575 (C═N), 1448, 1364, 1026. Anal. ($C_{12}H_{18}N_6 \cdot 1.2H_2O \cdot 0.2CH_3OH$) C, H, N, $C_{12}H_{18}N_6$ (246.31).

*(±)-2-Cyano-3-cyclopropyl-1-{[trans-3-(1H-imidazol-4-yl)-cyclopentyl]methyl}guanidine (**33**).* The title compound was prepared from **16** (0.05 g, 0.3 mmol) and **26** (0.061 g, 0.3 mmol) in MeCN (4.5 mL) according to the general procedure. Flash chromatography yielded a white solid (0.06 g, 74%); mp 43 °C. ^{1}H NMR (300 MHz, CD_3OD): δ [ppm] = 0.60 (m, 2H, cPr-CH_2), 0.83 (m, 2H, cPr-CH_2), 1.36 (m, 1H, CH_2), 1.68 (m, 1H, CH_2), 1.81 (m, 2H, CH_2), 1.93 (m, 1H, CH_2), 2.07 (m, 1H, CH_2), 2.39 (m, 1H, C*H*), 2.47 (m, 1H, cPr-C*H*), 3.17 (m, 1H, C*H*-Im), 3.22 (d, 2H, ^3J = 7.5 Hz, CH_2-N), 6.78 (s, 1H, Im-*H*-5), 7.56 (s, 1H, Im-*H*-2). ^{13}C NMR (75 MHz, CD_3OD): δ [ppm] = 8.12 (−, 2 cPr-CH_2), 23.77 (+, cPr-CH), 30.91 (−, CH_2), 33.91 (−, CH_2), 37.30 (−, CH_2), 37.76 (+, CH), 39.89 (+, CH), 47.51 (−, CH_2−N), 116.94 (+, Im-C-5), 120.11 (C_{quat},

DOI: 10.1021/acs.jmedchem.6b00120
J. Med. Chem. XXXX, XXX, XXX−XXX

C≡N), 135.70 (+, Im-C-2), 139.67 (C_{quat}, Im-C-4), 162.52 (C_{quat}, C=N). HRMS (EI-MS) calcd for $C_{14}H_{20}N_6$ [$M^{+\bullet}$] 272.1749; found 272.1743. IR (cm^{-1}) = 3261 (N-H), 2945, 2867 (C-H), 2160 (C≡N), 1570 (C=N), 1428, 1344, 1106. Anal. ($C_{14}H_{20}N_6 \cdot 0.4CH_3OH$) C, H, N, $C_{14}H_{20}N_6$ (272.35).

*(±)-2-Cyano-3-cyclopropyl-1-{[cis-3-(1H-imidazol-4-yl)-cyclopentyl]methyl}guanidine (**34**).* The title compound was prepared from **17** (0.05 g, 0.3 mmol) and **26** (0.061 g, 0.3 mmol) in MeCN (4.5 mL) according to the general procedure. Flash chromatography yielded a yellow solid (0.065 g, 80%); mp 46 °C. ^{1}H NMR (300 MHz, CD_3OD): δ [ppm] = 0.60 (m, 2H, cPr-CH_2), 0.82 (m, 2H, cPr-CH_2), 1.32 (m, 1H, CH_2), 1.50 (m, 1H, CH_2), 1.71 (m, 1H, CH_2), 1.83 (m, 1H, CH_2), 2.03 (m, 1H, CH_2), 2.18 (m, 1H, CH_2), 2.35 (m, 1H, CH), 2.47 (m, 1H, cPr-CH), 3.09 (m, 1H, CH-Im), 3.24 (m, 2H, CH_2-N), 6.78 (s, 1H, Im-H-5), 7.56 (s, 1H, Im-H-2). ^{13}C NMR (75 MHz, CD_3OD): δ [ppm] = 8.11 (−, 2 cPr-CH_2), 23.77 (+, cPr-CH), 30.01 (−, CH_2), 32.94 (−, CH_2), 38.79 (−, CH_2), 39.06 (+, CH), 40.93 (+, CH), 47.61 (−, CH_2−N), 116.78 (+, Im-C-5), 120.33 (C_{quat}, C≡N), 136.20 (+, Im-C-2), 141.88 (C_{quat}, Im-C-4), 162.49 (C_{quat}, C=N). IR (cm^{-1}) = 3253 (N-H), 2924, 2855 (C-H), 2161 (C≡N), 1575 (C=N), 1447, 1343, 1104. Anal. ($C_{14}H_{20}N_6 \cdot 0.35CH_3OH$) C, H, N, $C_{14}H_{20}N_6$ (272.35).

*(±)-2-Cyano-1-{[trans-3-(1H-imidazol-4-yl)cyclopentyl]methyl}-3-isobutylguanidine (**35**).* The title compound was prepared from **16** (0.05 g, 0.3 mmol) and **27** (0.066 g, 0.3 mmol) in MeCN (4.5 mL) according to the general procedure. Flash chromatography yielded a yellow solid (0.07 g, 81%); mp 47 °C. ^{1}H NMR (300 MHz, CD_3OD): δ [ppm] = 0.91 (d, 6H, ^3J = 6.7 Hz, 2 CH_3), 1.36 (m, 1H, CH_2), 1.63−1.87 (m, 4H, $CH(CH_3)_2$ + CH_2), 1.94 (m, 1H, CH_2), 2.07 (m, 1H, CH_2), 2.39 (m, 1H, CH), 3.01 (d, 2H, ^3J = 7.1 Hz, N-CH_2-$CH(CH_3)_2$), 3.17 (m, 1H, CH-Im), 3.18 (d, 2H, ^3J = 7.6 Hz, CH_2-N), 6.78 (s, 1H, Im-H-5), 7.57 (s, 1H, Im-H-2). ^{13}C NMR (75 MHz, CD_3OD): δ [ppm] = 20.31 (+, 2 CH_3), 29.60 (+, $CH(CH_3)_2$), 30.98 (−, CH_2), 33.86 (−, CH_2), 37.40 (−, CH_2), 37.80 (+, CH), 39.67 (+, CH), 47.73 (−, CH_2-N), 50.08 (−, N-CH_2-$CH(CH_3)_2$), 116.71 (+, Im-C-5), 120.29 (C_{quat}, C≡N), 135.09 (+, Im-C-2), 141.06 (C_{quat}, Im-C-4), 161.35 (C_{quat}, C=N). HRMS (EI-MS) calcd for $C_{15}H_{24}N_6$ [$M^{+\bullet}$] 288.2062; found 288.2057. IR (cm^{-1}) = 3266 (N-H), 2955, 2868 (C-H), 2156 (C≡N), 1576 (C=N), 1447, 1426, 1385, 1270, 1159, 1105. Anal. ($C_{15}H_{24}N_6 \cdot 0.5CH_3OH$) C, H, N. $C_{15}H_{24}N_6$ (288.39).

*(±)-2-Cyano-1-{[cis-3-(1H-imidazol-4-yl)cyclopentyl]methyl}-3-isobutylguanidine (**36**).* The title compound was prepared from **17** (0.05 g, 0.3 mmol) and **27** (0.066 g, 0.3 mmol) in MeCN (4.5 mL) according to the general procedure. Flash chromatography yielded a yellow solid (0.08 g, 92%); mp 62 °C. ^{1}H NMR (300 MHz, CD_3OD): δ [ppm] = 0.91 (d, 6H, ^3J = 6.7 Hz, 2 CH_3), 1.31 (m, 1H, CH_2), 1.50 (m, 1H, CH_2), 1.71 (m, 1H, CH_2), 1.85 (m, 2H, CH + CH_2), 2.03 (m, 1H, CH_2), 2.19 (m, 1H, CH_2), 2.33 (m, 1H, CH), 3.01 (d, 2H, ^3J = 7.2 Hz, N-CH_2-$CH(CH_3)_2$), 3.09 (m, 1H, CH-Im), 3.21 (d, 2H, ^3J = 8.3 Hz, CH_2-N), 6.78 (s, 1H, Im-H-5), 7.56 (s, 1H, Im-H-2). ^{13}C NMR (75 MHz, CD_3OD): δ [ppm] = 20.33 (+, 2 CH_3), 29.61 (+, $CH(CH_3)_2$), 30.12 (−, CH_2), 32.95 (−, CH_2), 38.82 (−, CH_2), 39.06 (+, CH), 40.74 (+, CH), 47.84 (−, CH_2-N), 50.09 (−, N-CH_2-$CH(CH_3)_2$), 116.82 (+, Im-C-5), 120.49 (C_{quat}, C≡N), 135.85 (+, Im-C-2), 140.41 (C_{quat}, Im-C-4), 161.33 (C_{quat}, C=N). HRMS (EI-MS) calcd for $C_{15}H_{24}N_6$ [$M^{+\bullet}$] 288.2062; found 288.2057. IR (cm^{-1}) = 3275 (N-H), 2956, 2868 (C-H), 2156 (C≡N), 1575 (C=N), 1449, 1426, 1384, 1270, 1157, 1107. Anal. ($C_{15}H_{24}N_6 \cdot 0.5CH_3OH$) C, H, N. $C_{15}H_{24}N_6$ (288.39).

*(±)-2-Cyano-1-{[trans-3-(1H-imidazol-4-yl)cyclopentyl]methyl}-3-(3-phenylpropyl)guanidine (**37**).* The title compound was prepared from **16** (0.04 g, 0.24 mmol) and **28** (0.068 g, 0.24 mmol) in MeCN (4.5 mL) according to the general procedure. Flash chromatography yielded a yellow solid (0.075 g, 89%); mp 50−51 °C. ^{1}H NMR (300 MHz, CD_3OD): δ [ppm] = 1.35 (m, 1H, CH_2), 1.69 (m, 1H, CH_2), 1.86 (m, 4H, CH_2 + CH_2-CH_2-Ph), 1.94 (m, 1H, CH_2), 2.08 (m, 1H, CH_2), 2.38 (m, 1H, CH), 2.64 (t, 2H, ^3J = 7.5 Hz, CH_2-Ph), 3.12−3.25 (m, 5H, CH-Im + N-CH_2 + CH_2-N), 6.85 (s, 1H, Im-H-5), 7.11−7.27 (m, 5H, Ph-H), 7.74 (s, 1H, Im-H-2). ^{13}C NMR (75 MHz, CD_3OD): δ [ppm] = 30.98 (−, CH_2), 32.30 (−, CH_2), 33.80 (−, CH_2), 33.99 (−, CH_2), 37.27 (−, CH_2), 37.49 (+, CH), 39.68 (+, CH), 42.38 (−, N-CH_2), 47.63 (−, CH_2-N), 116.57 (+, Im-C-5), 120.37 (C_{quat}, C≡N), 127.03 (+, Ph-C-4), 129.45 (+, 2 Ph-C), 129.51 (+, 2 Ph-C), 135.60 (+, Im-C-2), 139.37 (C_{quat}, Im-C-4), 142.86 (C_{quat}, Ph-C-1), 161.27 (C_{quat}, C=N). HRMS (EI-MS) calcd for $C_{20}H_{26}N_6$ [$M^{+\bullet}$] 350.2219; found 350.2212. IR (cm^{-1}) = 3262 (N-H), 2930, 2864 (C-H), 2158 (C≡N), 1574 (C=N), 1452, 1426, 1362, 1104. Anal. ($C_{20}H_{26}N_6 \cdot 0.6CH_3OH$) C, H, N. $C_{20}H_{26}N_6$ (350.46).

*(±)-2-Cyano-1-{[cis-3-(1H-imidazol-4-yl)cyclopentyl]methyl}-3-(3-phenylpropyl)guanidine (**38**).* The title compound was prepared from **17** (0.04 g, 0.24 mmol) and **28** (0.068 g, 0.24 mmol) in MeCN (4.5 mL) according to the general procedure. Flash chromatography yielded a yellow solid (0.06 g, 72%); mp 53−54 °C. ^{1}H NMR (300 MHz, CD_3OD): δ [ppm] = 1.31 (m, 1H, CH_2), 1.49 (m, 1H, CH_2), 1.70 (m, 1H, CH_2), 1.85 (m, 1H, CH_2), 1.86 (m, 2H, CH_2-CH_2-Ph), 2.03 (m, 1H, CH_2), 2.18 (m, 1H, CH_2), 2.31 (m, 1H, CH), 2.64 (t, 2H, ^3J = 7.6 Hz, CH_2-Ph), 3.09 (m 1H, CH-Im), 3.16−3.24 (m, 4H, N-CH_2 + CH_2-N), 6.79 (s, 1H, Im-H-5), 7.11−7.27 (m, 5H, Ph-H), 7.58 (s, 1H, Im-H-2). ^{13}C NMR (75 MHz, CD_3OD): δ [ppm] = 30.10 (−, CH_2), 32.31 (−, CH_2), 32.93 (−, CH_2), 33.99 (−, CH_2), 38.84 (−, CH_2), 39.05 (+, CH), 40.73 (+, CH), 42.38 (−, N-CH_2), 47.80 (−, CH_2-N), 118.69 (+, Im-C-5), 120.98 (C_{quat}, C≡N), 127.02 (+, Ph-C-4), 129.45 (+, 2 Ph-C), 129.50 (+, 2 Ph-C), 135.57 (+, Im-C-2), 140.71 (C_{quat}, Im-C-4), 142.86 (C_{quat}, Ph-C-1), 161.25 (C_{quat}, C=N). HRMS (EI-MS) calcd for $C_{20}H_{26}N_6$ [$M^{+\bullet}$] 350.2219; found 350.2212. IR (cm^{-1}) = 3259 (N-H), 2939, 2864 (C-H), 2158 (C≡N), 1575 (C=N), 1451, 1426, 1362, 1104. Anal. ($C_{20}H_{26}N_6 \cdot 0.55CH_3OH$) C, H, N. $C_{20}H_{26}N_6$ (350.46).

*(±)-2-Cyano-1-{[trans-3-(1H-imidazol-4-yl)cyclopentyl]methyl}-3-[2-(phenylsulfanyl)ethyl]guanidine (**39**).* The title compound was prepared from **16** (0.04 g, 0.24 mmol) and **29** (0.072 g, 0.24 mmol) in MeCN (4.5 mL) according to the general procedure. Flash chromatography yielded a white solid (0.08 g, 90%); mp 46−47 °C. ^{1}H NMR (300 MHz, CD_3OD): δ [ppm] = 1.32 (m, 1H, CH_2), 1.73 (m, 2H, CH_2), 1.82 (m, 1H, CH_2), 1.94 (m, 1H, CH_2), 2.06 (m, 1H, CH_2), 2.35 (m, 1H, CH), 3.11 (m, 5H, CH-Im + N-CH_2 + CH_2-N), 3.41 (m, 2H, CH_2-S), 6.77 (s, 1H, Im-H-5), 7.17 (m, 1H, Ph-H-4), 7.28 (m, 2H, Ph-H), 7.37 (m, 2H, Ph-H), 7.57 (s, 1H, Im-H-2). ^{13}C NMR (75 MHz, CD_3OD): δ [ppm] = 31.01 (−, CH_2), 33.61 (−, CH_2−S), 33.85 (−, CH_2), 37.37 (−, CH_2), 37.74 (+, CH), 39.47 (+, CH), 42.27 (−, N-CH_2), 47.82 (−, CH_2-N), 116.69 (+, Im-C-5), 119.99 (C_{quat}, C≡N), 127.34 (+, Ph-C-4), 130.16 (+, 2 Ph-C), 130.46 (+, 2 Ph-C), 135.92 (+, Im-C-2), 136.99 (C_{quat}, Ph-C-1), 141.87 (C_{quat}, Im-C-4), 161.18 (C_{quat}, C=N). HRMS (EI-MS) calcd for $C_{19}H_{24}N_6S$ [$M^{+\bullet}$] 368.1783; found 368.1778. IR (cm^{-1}) = 3255 (N-H), 2946, 2864 (C-H), 2159 (C≡N), 1574 (C=N), 1437, 1357, 1300, 1088. Anal. ($C_{19}H_{24}N_6S \cdot 0.3CH_3OH$) C, H, N. $C_{19}H_{24}N_6S$ (368.50).

*(±)-2-Cyano-1-{[cis-3-(1H-imidazol-4-yl)cyclopentyl]methyl}-3-[2-(phenylsulfanyl)ethyl]guanidine (**40**).* The title compound was prepared from **17** (0.04 g, 0.24 mmol) and **29** (0.072 g, 0.24 mmol) in MeCN (4.5 mL) according to the general procedure. Flash chromatography yielded a yellow solid (0.06 g, 68%); mp 48−49 °C. ^{1}H NMR (300 MHz, CD_3OD): δ [ppm] = 1.31 (m, 1H, CH_2), 1.47 (m, 1H, CH_2), 1.71 (m, 1H, CH_2), 1.84 (m, 1H, CH_2), 2.02 (m, 1H, CH_2), 2.20 (m, 1H, CH_2), 2.29 (m, 1H, CH), 3.10 (m, 5H, CH-Im + N-CH_2 + CH_2-N), 3.41 (t, 2H, ^3J = 7.3 Hz, CH_2-S), 6.78 (s, 1H, Im-H-5), 7.18 (t, 1H, ^3J = 7.6 Hz, Ph-H-4), 7.29 (m, 2H, Ph-H-3,5), 7.57 (s, 1H, Im-H-2), 8.08 (d, 2H, ^3J = 8.1 Hz, Ph-H-2,6). ^{13}C NMR (75 MHz, CD_3OD): δ [ppm] = 30.11 (−, CH_2), 32.92 (−, CH_2), 33.60 (−, CH_2−S), 38.79 (−, CH_2), 38.98 (+, CH), 40.54 (+, CH), 42.28 (−, N-CH_2), 47.90 (−, CH_2−N), 116.53 (+, Im-C-5), 120.00 (C_{quat}, C≡N), 127.34 (+, Ph-C-4), 130.16 (+, 2 Ph-C), 130.44 (+, 2 Ph-C), 135.87 (+, Im-C-2), 137.01 (C_{quat}, Ph-C-1), 141.68 (C_{quat}, Im-C-4), 161.16 (C_{quat}, C=N). HRMS (EI-MS) calcd for $C_{19}H_{24}N_6S$ [$M^{+\bullet}$] 368.1783; found 368.1774. IR (cm^{-1}) = 3243 (N-H), 2925, 2855 (C-H), 2158 (C≡N), 1572 (C=N), 1436, 1355, 1300, 1088. Anal. ($C_{19}H_{24}N_6S \cdot 0.4CH_3OH$) C, H, N. $C_{19}H_{24}N_6S$ (368.50).

*(±)-2-Cyano-1-{[trans-3-(1H-imidazol-4-yl)cyclopentyl]methyl}-3-[2-(phenoxy)ethyl]guanidine (**41**).* The title compound was

DOI: 10.1021/acs.jmedchem.6b00120
J. Med. Chem. XXXX, XXX, XXX−XXX

prepared from **16** (0.04 g, 0.24 mmol) and **30** (0.068 g, 0.24 mmol) in MeCN (4.5 mL) according to the general procedure. Flash chromatography yielded a white solid (0.05 g, 59%); mp 55 °C. ^{1}H NMR (300 MHz, CD_3OD): δ [ppm] = 1.33 (m, 1H, CH_2), 1.65 (m, 1H, CH_2), 1.82 (m, 2H, CH_2), 1.93 (m, 1H, CH_2), 2.05 (m, 1H, CH_2), 2.38 (m, 1H, CH), 3.15 (m, 1H, CH-Im), 3.19 (d, 2H, ^3J = 7.5 Hz, CH_2-N), 3.61 (t, 2H, ^3J = 5.4 Hz, N-CH_2), 4.07 (t, 2H, ^3J = 5.4 Hz, CH_2-O), 6.75 (s, 1H, Im-*H*-5), 6.89−6.94 (m, 3H, Ph-*H*), 7.25 (m, 2H, Ph-*H*), 7.57 (s, 1H, Im-*H*-2). ^{13}C NMR (75 MHz, CD_3OD): δ [ppm] = 31.03 (−, CH_2), 33.87 (−, CH_2), 37.33 (−, CH_2), 37.69 (+, CH), 39.64 (+, CH), 42.45 (−, N-CH_2), 47.79 (−, CH_2-N), 67.67 (−, CH_2-O), 115.64 (+, 2 Ph-*C*), 116.72 (+, Im-*C*-5), 120.06 (C_{quat}, *C*≡N), 122.15 (+, Ph-*C*-4), 130.59 (+, 2 Ph-*C*), 135.87 (+, Im-*C*-2), 142.10 (C_{quat}, Im-*C*-4), 160.11 (C_{quat}, Ph-*C*-1), 161.54 (C_{quat}, *C*═N). HRMS (EI-MS) calcd for $C_{19}H_{24}N_6O$ [$M^{+\bullet}$] 352.2012; found 352.2007. IR (cm^{-1}) = 3256 (N-H), 2971, 2901 (C-H), 2162 (C≡N), 1578 (C═N), 1406, 1241, 1071, 1049. Anal. ($C_{19}H_{24}N_6O$·0.5CH_3OH) C, H, N. $C_{19}H_{24}N_6O$ (352.43).

*(±)-2-Cyano-1-{[cis-3-(1H-imidazol-4-yl)cyclopentyl]methyl}-3-[2-(phenoxy)ethyl]guanidine (**42**).* The title compound was prepared from **17** (0.04 g, 0.24 mmol) and **30** (0.068 g, 0.24 mmol) in MeCN (4.5 mL) according to the general procedure. Flash chromatography yielded a yellow solid (0.05 g, 59%); mp 57 °C. ^{1}H NMR (300 MHz, CD_3OD): δ [ppm] = 1.30 (m, 1H, CH_2), 1.49 (m, 1H, CH_2), 1.70 (m, 1H, CH_2), 1.83 (m, 1H, CH_2), 2.00 (m, 1H, CH_2), 2.18 (m, 1H, CH_2), 2.31 (m, 1H, CH), 3.06 (m, 1H, CH-Im), 3.21 (d, 2H, ^3J = 7.0 Hz, CH_2-N), 3.61 (t, 2H, ^3J = 5.3 Hz, N-CH_2), 4.07 (t, 2H, ^3J = 5.3 Hz, CH_2-O), 6.76 (s, 1H, Im-*H*-5), 6.92 (m, 3H, Ph-*H*), 7.25 (m, 2H, Ph-*H*), 7.56 (s, 1H, Im-*H*-2). ^{13}C NMR (75 MHz, CD_3OD): δ [ppm] = 30.10 (−, CH_2), 32.91 (−, CH_2), 38.81 (−, CH_2), 38.95 (+, CH), 40.68 (+, CH), 42.45 (−, N-CH_2), 47.87 (−, CH_2-N), 67.66 (−, CH_2-O), 115.64 (+, 2 Ph-*C*), 116.62 (+, Im-*C*-5), 120.23 (C_{quat}, *C*≡N), 122.14 (+, Ph-*C*-4), 130.59 (+, 2 Ph-*C*), 135.88 (+, Im-*C*-2), 142.04 (C_{quat}, Im-*C*-4), 160.13 (C_{quat}, Ph-*C*-1), 161.52 (C_{quat}, C═N). HRMS (EI-MS) calcd for $C_{19}H_{24}N_6O$ [$M^{+\bullet}$] 352.2012; found 352.2008. IR (cm^{-1}) = 3257 (N-H), 2924, 2868 (C-H), 2160 (C≡N), 1576 (C═N), 1453, 1239, 1080, 1050. Anal. ($C_{19}H_{24}N_6O$·0.5CH_3OH) C, H, N. $C_{19}H_{24}N_6O$ (352.43).

*(±)-2-Cyano-1-{[trans-3-(1H-imidazol-4-yl)cyclopentyl]methyl}-3-[2-(phenylamino)ethyl]guanidine (**46**).* The title compound was prepared from **43** (0.08 g, 0.26 mmol) and N^1-phenylethane-1,2-diamine (**45**) (0.034 mL, 0.26 mmol) in MeCN (4.5 mL) according to the general procedure. Flash chromatography yielded a white solid (0.05 g, 55%); mp 42−43 °C. ^{1}H NMR (300 MHz, CD_3OD): δ [ppm] = 1.31 (m, 1H, CH_2), 1.58−1.84 (m, 3H, CH_2), 1.90 (m, 1H, CH_2), 2.05 (m, 1H, CH_2), 2.32 (m, 1H, CH), 3.14 (m, 3H, CH-Im + CH_2-N), 3.27 (t, 2H, ^3J = 6.2 Hz, N-CH_2), 3.41 (t, 2H, ^3J = 6.2 Hz, CH_2-NH-Ph), 6.63 (m, 3H, Ph-*H*), 6.79 (s, 1H, Im-*H*-5), 7.09 (m, 2H, Ph-*H*), 7.66 (s, 1H, Im-*H*-2). ^{13}C NMR (75 MHz, CD_3OD): δ [ppm] = 31.00 (−, CH_2), 33.83 (−, CH_2), 37.27 (−, CH_2), 37.57 (+, CH), 39.52 (+, CH), 42.47 (−, N-CH_2), 44.47 (−, CH_2-NH-Ph), 47.78 (−, CH_2-N), 114.00 (+, 2 Ph-*C*), 116.53 (+, Im-*C*-5), 118.34 (+, Ph-*C*-4), 120.23 (C_{quat}, *C*≡N), 130.21 (+, 2 Ph-*C*), 135.80 (+, Im-*C*-2), 141.86 (C_{quat}, Im-*C*-4), 149.85 (C_{quat}, Ph-*C*-1), 161.61 (C_{quat}, C═N). HRMS (LSI-MS (MeOH/glycerol)) calcd for $C_{19}H_{26}N_7$ [M + H]$^+$ 352.2250; found 352.2249. IR (cm^{-1}) = 3264 (N-H), 2930, 2864 (C-H), 2159 (C≡N), 1575 (C═N), 1499, 1426, 1323, 1257. Anal. ($C_{19}H_{25}N_7$·0.75CH_3OH) C, H, N. $C_{19}H_{25}N_7$ (351.45).

*(±)-2-Cyano-1-{[cis-3-(1H-imidazol-4-yl)cyclopentyl]methyl}-3-[2-(phenylamino)ethyl]guanidine (**47**).* The title compound was prepared from **44** (0.09 g, 0.29 mmol) and **45** (0.038 mL, 0.29 mmol) in MeCN (4.5 mL) according to the general procedure. Flash chromatography yielded a pale-yellow solid (0.07 g, 69%); mp 55−57 °C. ^{1}H NMR (300 MHz, CD_3OD): δ [ppm] = 1.30 (m, 1H, CH_2), 1.45 (m, 1H, CH_2), 1.68 (m, 1H, CH_2), 1.80 (m, 1H, CH_2), 2.01 (m, 1H, CH_2), 2.14 (m, 1H, CH_2), 2.24 (m, 1H, CH), 3.05 (m, 1H, CH-Im) 3.15 (d, 2H, ^3J = 8.4 Hz, CH_2-N), 3.27 (t, 2H, ^3J = 5.9 Hz, N-CH_2), 3.41 (t, 2H, ^3J = 5.9 Hz, CH_2-NH-Ph), 6.63 (m, 3H, Ph-*H*), 6.76 (s, 1H, Im-*H*-5), 7.09 (m, 2H, Ph-*H*), 7.57 (s, 1H, Im-*H*-2). ^{13}C NMR (75 MHz, CD_3OD): δ [ppm] = 30.10 (−, CH_2), 32.90 (−, CH_2), 38.80 (−, CH_2), 38.92 (+, CH), 40.59 (+, CH), 42.46 (−, N-CH_2), 44.46 (−, CH_2-NH-Ph), 47.90 (−, CH_2-N), 113.98 (+, 2 Ph-*C*), 116.56 (+, Im-*C*-5), 118.34 (+, Ph-*C*-4), 120.23 (C_{quat}, *C*≡N), 130.21 (+, 2 Ph-*C*), 135.86 (+, Im-*C*-2), 141.92 (C_{quat}, Im-*C*-4), 149.84 (C_{quat}, Ph-*C*-1), 161.58 (C_{quat}, *C*═N). HRMS (LSI-MS (MeOH/glycerol)) calcd for $C_{19}H_{26}N_7$ [M + H]$^+$ 352.2250; found 352.2242. IR (cm^{-1}) = 3275 (N-H), 2971, 2901 (C-H), 2161 (C≡N), 1577 (C═N), 1499, 1406, 1251. Anal. ($C_{19}H_{25}N_7$·0.7CH_3OH) C, H, N. $C_{19}H_{25}N_7$ (351.45).

Chiral Separation by HPLC. Preparative HPLC was performed at room temperature with a system from Knauer (Berlin, Germany) consisting of two K-1800 pumps, a K-2001 detector (UV detection at 220 nm), and a chiral NP-column (Chiralcel OJ-H, 250 mm × 20 mm, 5 μm, Daicel Chemical Industries Ltd., Fort Lee, NJ, USA) at a flow rate of 18 mL/min. Mixtures of heptane and 2-propanol (85/15, v/v, isocratic elution) were used as mobile phase. Solvents were removed from the eluates under reduced pressure (final pressure: 60 mbar) at 40 °C prior to lyophilization. Chiral analytical HPLC analysis was performed on a system from Varian (Varian 920-LC, Darmstadt, Germany) and a NP-column thermostated at 30 °C (Chiralcel OJ-H, 250 mm × 4.6 mm, 5 μm, Daicel Chemical Industries Ltd., Fort Lee, NJ, USA; t_0 = 3.02 min) at a flow rate of 1.0 mL/min. UV-detection was done at 215 nm. Mixtures of heptane and 2-propanol (**31**:**32**: 85/15, v/v; **39**:**40**: 80/20, v/v; isocratic elution) were used as mobile phase. helium degassing was used throughout. Compound purities were calculated as percentage peak area of the analyzed compound by UV detection at 215 nm. Purity of tested compounds was >95% for all compounds as determined by HPLC. Optical rotations were measured on a PerkinElmer 141 polarimeter in the specified solvent. Concentrations are indicated in [g/100 mL]. Circular dichroism was determined with a Jasco CD1595 spectropolarimeter (Jasco GmbH, Groß-Umstadt, Germany) directly coupled to analytical HPLC at 240 nm at room temperature.

Separated enantiomers (data cf. Table 1): (−)-2-Cyano-1-{[*trans*-(1*R*,3*R*)-3-(1*H*-imidazol-4-yl)cyclopentyl]methyl}-3-methylguanidine (**31a**), (+)-2-cyano-1-{[*trans*-(1*S*,3*S*)-3-(1*H*-imidazol-4-yl)-cyclopentyl]methyl}-3-methylguanidine (**31b**), (−)-2-cyano-1-{[*cis*-(1*S*,3*R*)-3-(1*H*-imidazol-4-yl)cyclopentyl]methyl}-3-methylguanidine (**32a**), (+)-2-cyano-1-{[*cis*-(1*R*,3*S*)-3-(1*H*-imidazol-4-yl)cyclopentyl]-methyl}-3-methylguanidine (**32b**), (+)-2-cyano-1-{[*trans*-(1*S*,3*S*)-3-(1*H*-imidazol-4-yl)cyclopentyl]methyl}-3-[2-(phenylsulfanyl)ethyl]-guanidine (**39a**), (−)-2-cyano-1-{[*trans*-(1*R*,3*R*)-3-(1*H*-imidazol-4-yl)cyclopentyl]methyl}-3-[2-(phenylsulfanyl)ethyl]guanidine (**39b**), (−)-2-cyano-1-{[*cis*-(1*S*,3*R*)-3-(1*H*-imidazol-4-yl)cyclopentyl]-methyl}-3-[2-(phenylsulfanyl)ethyl]guanidine (**40a**), (+)-2-cyano-1-{[*cis*-(1*R*,3*S*)-3-(1*H*-imidazol-4-yl)cyclopentyl]methyl}-3-[2-(phenylsulfanyl)ethyl]guanidine (**40b**).

Pharmacological Methods. *Materials.* Histamine dihydrochloride was purchased from Alfa Aesar (Karlsruhe, Germany), Iodophenpropit (**61**) from Tocris Bioscience (Ellisville, USA), [^{3}H]mepyramine ([^{3}H]**64**), [^{3}H]tiotidine ([^{3}H]**65**), [^{3}H]N^α-methylhistamine ([^{3}H]**66**), and [^{3}H]histamine were from PerkinElmer Life Sciences (Boston, MA). The compounds **1**,[37] **58**,[65] **59**,[58] **60**,[60] [^{3}H]**60**,[59] **62**,[66] and **63**[67] were synthesized according to reported protocols. [γ-^{32}P]GTP was synthesized according to a previously described method.[68] [^{32}P]P_i (8500−9100 Ci/mmol orthophosphoric acid) was from PerkinElmer Life Sciences (Boston, MA, USA). Guanosine diphosphate (GDP) and polyethylenimine were from Sigma-Aldrich Chemie GmbH (Munich, Germany), and unlabeled GTPγS was from Roche (Mannheim, Germany). [^{35}S]GTPγS was from PerkinElmer Life Sciences (Boston, MA) or Hartmann Analytic GmbH (Braunschweig, Germany). GF/C filters were from Whatman Ltd. (Maidstone, UK). Glycerol-3-phosphate dehydrogenase, triose phosphate isomerase, glyceraldehyde-3-phosphate dehydrogenase, and lactate dehydrogenase were from Roche (Mannheim, Germany). 3-Phosphoglycerate kinase, L-α-glycerol phosphate, tricine, ethylene glycol tetraacetic acid (EGTA), dithiothreitol (DTT), glycylglycine, forskolin, DMEM, and adenosine triphosphate were from Sigma-Aldrich Chemie GmbH (Munich, Germany). Fetal bovine serum (FBS) and the antibiotic G418 were from Biochrom AG (Berlin,

DOI: 10.1021/acs.jmedchem.6b00120
J. Med. Chem. XXXX, XXX, XXX−XXX

Germany). Hygromycin B was from MoBiTec GmbH (Göttingen, Germany). Triton-X was from Serva Electrophoresis GmbH (Heidelberg, Germany). D-Luciferin potassium salt was from Synchem OHG (Felsberg, Germany). Culture flasks were from Nunc GmbH (Wiesbaden, Germany).

Cells. Sf9 insect cells were from BD Biosciences (BD Biosciences, Heidelberg, Germany), and human embryonal kidney cells (HEK-293 cells) were from Deutsche Sammlung für Mikroorganismen and Zellkulturen (DSMZ, Braunschweig, Germany). The genetically engineered cells used to perform the functional and binding studies described in this study were generated and maintained as described (cf. brief description of protocols and references cited below). Examination for mycoplasma contamination was routinely performed using the Venor GeM mycoplasma detection kit (Minerva Biolabs, Berlin, Germany) and was negative for all cell types.

[^{35}S]GTPγS Binding Assay.[69,70] [^{35}S]GTPγS binding assays were performed as previously described for the H_2R,[71,72] H_3R,[73,74] and H_4R.[75] H_2R assays: Sf9 insect cell membranes expressing the hH_2R-$Gs\alpha_S$ fusion protein were employed. H_3R assays: Sf9 insect cell membranes coexpressing the hH_3R, mammalian $G\alpha_{i2}$ and $G\beta_1\gamma_2$ were employed. H_4R assays: Sf9 insect cell membranes coexpressing the hH_4R, mammalian $G\alpha_{i2}$ and $G\beta_1\gamma_2$ were employed.

The respective membranes were thawed and sedimented by a 10 min centrifugation at 4 °C and 13000*g*. Membranes were resuspended in binding buffer (12.5 mM $MgCl_2$, 1 mM EDTA, and 75 mM Tris/HCl, pH 7.4). Each assay tube contained Sf9 membranes expressing the respective HR subtype (15−30 μg protein/tube), 1 μM GDP, 0.05% (w/v) bovine serum albumin, 0.2 nM [^{35}S]GTPγS, and the investigated ligands (dissolved in Millipore water or in a mixture (v/v) of 80% Millipore water and 20% DMSO) at various concentrations in binding buffer (total volume 250 μL). All H_4R assays additionally contained 100 mM NaCl. For the determination of K_B values (antagonist mode of the [^{35}S]GTPγS binding assay), histamine was added to the reaction mixtures (final concentrations: H_2R, 1 μM; $H_3/_4R$, 100 nM). Incubations were conducted for 90 min at 25 °C and shaking at 250 rpm. Bound [^{35}S]GTPγS was separated from free [^{35}S]GTPγS by filtration through GF/C filters, followed by three washes with 2 mL of binding buffer (4 °C) using a Brandel harvester. Filter-bound radioactivity was determined after an equilibration phase of at least 12 h by liquid scintillation counting. The experimental conditions chosen ensured that no more than 10% of the total amount of [^{35}S]GTPγS added was bound to filters. Nonspecific binding was determined in the presence of 10 μM unlabeled GTPγS.

Steady-State GTPase Activity Assay. GTPase activity assays were performed as previously described.[75−79] H_1R assays: Sf9 insect cell membranes coexpressing the hH_1R and RGS4 were employed. H_2R assays: Sf9 insect cell membranes expressing the hH_2R-$Gs\alpha_S$ fusion protein were used. H_3R assays: Sf9 insect cell membranes coexpressing the hH_3R, and mammalian $G\alpha_{i2}$, $G\beta_1\gamma_2$ and RGS4 were employed. H_4R assays: Sf9 insect cell membranes coexpressing the hH_4R-GAIP fusion protein, and mammalian $G\alpha_{i2}$ and $G\beta_1\gamma_2$ were used. The respective membranes were thawed and sedimented by centrifugation at 4 °C and 13000*g* for 10 min. Membranes were resuspended in 10 mM Tris/HCl, pH 7.4. Each assay tube contained Sf9 membranes expressing the respective HR subtype (10−20 μg protein/tube), $MgCl_2$ ($H_{1,2}R$ assays, 1.0 mM; $H_{3,4}R$ assays, 5.0 mM), 100 μM EDTA, 100 μM ATP, 100 nM GTP, 100 μM adenylyl imidophosphate, 5 mM creatine phosphate, 40 μg creatine kinase, and 0.2% (w/v) bovine serum albumin in 50 mM Tris/HCl, pH 7.4, and the investigated ligands at various concentrations. All H_4R assays additionally contained 100 mM NaCl. For the determination of pK_B values (antagonist mode of the GTPase activity assay), histamine was added to the reaction mixtures (final concentrations: H_1R, 200 nM; H_2R, 1 μM; $H_{3,4}R$, 100 nM). Reaction mixtures (80 μL) were incubated for 2 min at 25 °C. After the addition of 20 μL of [γ-^{32}P]GTP (0.1 μCi/tube), reaction mixtures were incubated for 20 min at 25 °C. Reactions were terminated by the addition of 900 μL of slurry consisting of 5% (w/v) activated charcoal and 50 mM NaH_2PO_4, pH 2.0. Charcoal absorbs nucleotides but not P_i. Charcoal-quenched reaction mixtures were centrifuged for 7 min at room temperature at 13000*g*. Then 600 μL of the supernatant were removed and $^{32}P_i$ was determined by liquid scintillation counting. Spontaneous [γ-^{32}P]GTP degradation was determined in tubes containing all components described above plus a high concentration of unlabeled GTP (1 mM) that due to competition with [γ-^{32}P]GTP prevents [γ-^{32}P]GTP hydrolysis by enzymatic activities present in Sf9 membranes. Spontaneous [γ-^{32}P]GTP degradation was <1% of the total amount of radioactivity added. The experimental conditions chosen ensured that not more than 10% of the total amount of [γ-^{32}P]GTP added was converted to $^{32}P_i$.

Radioligand Binding Assays..[78,80] For the binding experiments the Sf9 insect cell membranes described above were employed. The respective membranes were thawed and sedimented by centrifugation at 4 °C and 13000*g* for 10 min. Membranes were resuspended in binding buffer (12.5 mM $MgCl_2$, 1 mM EDTA, and 75 mM Tris/HCl, pH 7.4). Each tube (total volume 500 μL) contained 50 μg (hH_1R, hH_3R), 120 μg (hH_4R), or 250 μg (hH_2R) of membrane protein. Competition binding experiments were performed in the presence of 5 nM [^{3}H]mepyramine (hH_1R), 10 nM [^{3}H]tiotidine (hH_2R), 3 nM [^{3}H]N^α-methylhistamine (hH_3R), or 10 nM [^{3}H]histamine or 3 nM [^{3}H]**60** (hH_4R) and increasing concentrations of unlabeled ligands. Incubations were conducted for 60 min at 25 °C and shaking at 250 rpm. Bound radioligand was separated from free radioligand by filtration through 0.3% polyethylenimine-pretreated (PEI) GF/C filters, followed by three washes with 2 mL of cold binding buffer (4 °C) using a Brandel harvester. Filter-bound radioactivity was determined after an equilibration phase of at least 12 h by liquid scintillation counting.

Luciferase Reporter Gene Assay. The assay was performed as previously described.[33] In brief, HEK293-SF-hH_4R-His_6-CRE-luc or HEK293-SF-mH_4R-His_6-CRE-Luc cells were cultured in DMEM supplemented with 10% FBS and selection antibiotics (600 μg/mL G418 and 200 μg/mL hygromycin B) in a water-saturated atmosphere containing 5% CO_2 at 37 °C. Cells were passaged (1:10) twice a week. For the assay, approximately 2×10^5 cells/well were seeded in 96-well plates in DMEM + 10% FBS 17 h before the assay. After addition of increasing concentrations of histaminergic ligands and forskolin (400 nM (hH_4R) or 1 μM (mH_4R)), the cells were incubated for 5 h. Thereafter, the medium was discarded, the cells were washed with cold PBS, and lysed in 40 μL of lysis buffer (25 mM tricine, pH 7.8, 10% (v/v) glycerol, 2 mM EGTA, 1% (v/v) Triton X-100, 5 mM $MgSO_4 \cdot 7H_2O$, 1 mM DTT) under shaking (180 rpm) for 30 min. Luminescence was measured with a Tecan GENios Pro microplate reader by injection of 80 μL of D-luciferin solution (0.2 mg/mL D-luciferin potassium salt, 25 mM glycylglycine, 15 mM $MgSO_4 \cdot 7H_2O$, 15 mM KH_2PO_4, pH 7.8, 4 mM EGTA, pH 7.8, 2 mM ATP, and 2 mM DTT) to 20 μL of the lysate.

Data Analysis and Pharmacological Parameters. All data are presented as mean of *N* independent experiments ± SEM. Agonist potencies were given as EC_{50} values (molar concentration of the agonist causing 50% of the maximal response). Maximal responses (intrinsic activities) were expressed as α values. The α value of histamine was set to 1.00, and α values of other compounds were referred to this value.

IC_{50} values were converted to K_i and K_B values using the Cheng−Prussoff equation.[81] K_i values were analyzed by nonlinear regression and best fit to one-site (monophasic) competition isotherms. EC_{50} and K_B values from the functional [^{35}S]GTPγS, GTPase, and luciferase gene reporter assays were analyzed by nonlinear regression and best fit to sigmoidal dose−response curves (GraphPad Prism 5.0 software, San Diego, CA).

Molecular Modeling. *Inactive-State Model of the hH_4R.* The crystal structure of hH_1R 3RZE,[82] with the antagonist doxepine bound, was used as a template to construct the inactive state of hH_4R by homology modeling, as already described.[83] Briefly, the lysozyme, which was artificially cocrystallized in 3RZE, was deleted. The E2-loop is not completely available in the hH_1R crystal. Thus, for modeling of the E2-loop, the amino acids Trp^{165}, Asn^{166}, and His^{167} of the hH_1R crystal were removed at first. Afterward, the missing amino acids (hH_4R: Val^{153}-Lys^{158}) were included into the models, using the "Loop-

DOI: 10.1021/acs.jmedchem.6b00120
J. Med. Chem. XXXX, XXX, XXX−XXX

Search" module from SYBYL 7.0 (Tripos Inc.). The N-Terminus, which is also missing in the crystal structure, was added using SYBYL 7.0 (Tripos Inc.) according to the following protocol:[84] The first 15 (hH_4R) amino acids of the N-terminus were added to the receptor models with SYBYL, using a random conformation for the backbone. Afterward, position restraints were set onto the whole inactive receptor model except the added amino acids of the N-terminus and the amino acids of the E2-loop, added by Loop-Search, as described above. The structures were energetically minimized using SYBYL. Subsequently, short gas phase MD simulations (500 ps) of the N-terminus and inserted amino acids of the E2-loop with the same positions restraints, as used for the minimization, were performed. The resulting model for the inactive hH_4R was used for insertion of the missing I3-loop. Because of the lack of information concerning the conformation of the long I3-loop of the hH_4R, the amino acids Gly^{215} to His^{292} (hH_4R) were not included in the models. To close the gap between the intracellular parts of TM V and TM VI, eight alanines were inserted instead at hH_4R. It was shown that internal water molecules play an important role in stabilization or activation of aminergic GPCRs.[85,86] Thus, these internal water molecules were included into the model of inactive hH_4R based on the 2RH1 crystal structure.[82] The compounds **39a** and **39b**, with a positively charged histamine moiety, were docked manually into the orthosteric binding pocket of the hH_4R in an analogous manner as described previous.[37] The force field parameters of the compounds were obtained from the PRODRG server (http://davapc1.bioch.dundee.ac.uk/prodrg/).[87] The partial charges according to Gasteiger and Hückel, calculated by SYBYL, were assigned to **39a** and **39b**. The resulting complex was energetically minimized. Afterward, the minimized receptor model was embedded into a POPC lipid bilayer, as described previously.[83] Intracellular and extracellular water, as well as an appropriate number of sodium and chloride ions, were added into the simulation box and the molecular dynamic simulations, using GROMACS 4.0.2 (http://www.gromacs.org), were performed as already described.[83] For the POPC lipid, the force field parameters available at an appropriate online source (http://moose.bio.ucalgary.ca/index.php?page=Structures_and_Topologies) were used. Subsequent to a 5 ns equilibration phase for each system (force constants (250 kJ/(mol nm^2) for the first 2.5 ns and 100 kJ/(mol nm^2) for the second 2.5 ns) were put onto the backbone atoms of the TM domains of hH_4R), and the 50 ns productive phases were performed.

Active-State Model of hH_4R-G$\alpha i2\beta\gamma$. The active state model of the hH_4R–G$\alpha i\beta\gamma$-complex was modeled by homology modeling based on the crystal structure of the $h\beta_2R$–G$\alpha s\beta\gamma$ complex (3SN6).[88] The hH_4R within this complex was modeled in an analogous manner to the inactive model of the hH_4R as described above and **39a** was docked as described above. The homology modeling of the Gα-subunit is based on the amino acid alignment between Gαs and Gαi2 (cf. Supporting Information) and was performed with SYBYL according the following protocol: The following sequences were directly mutated (Gαs → Gαi2): 9–59 → 2–52, 88–202 → 66–180, 205–255 → 183–233, 263–301 → 241–279, 306–308 → 282–284, 335–350 → 293–308, 354–355 → 316-317, and 361–394 → 322–355. The missing amino acid Met^1 was added. The amino acids 181–182 and 234–240 were added by loop search because the corresponding amino acids were missing in the 3SN6 crystal. The amino acids Met^{60}-Glu^{88} of the Gαs subunit were also missing in the 3SN6 crystal, thus the amino acids 53–65 were also added by loop search. Because the loop search of loops >10 amino acids may lead to structural uncertainties, the loop which was most similar to the corresponding part of the crystal structure of Gαi1 (1GP2)[89] was included into the homology model. Because of the different numbers of amino acids, the amino acids 302–305 of the Gαs-subunit in the 3SN6 crystal were deleted and the amino acids Thr^{280}-His^{281} of Gαi2 were included by loop search. The alignment (cf. Supporting Information) shows that the corresponding regions 309–334 (Gαs) → 285–292 (Gαi2), 351–353 (Gαs) → 309–315 (Gαi2), and 356–360 (Gαs) → 318–321 (Gαi2) between Gαs and Gαi2 are of different length. Thus, instead of a direct homology modeling, the amino acids 309–334, 351–353, and 356–360 of the Gαs-subunit of the 3SN6 crystal were deleted. The amino acids 285–292 (Gαi2), 309–315 (Gαi2), and 318–321 (Gαi2) were included by loops search. The loops 285–292 (Gαi2) and 309–315 (Gαi2) were chosen that were most similar to the corresponding structures of Gαi1 (1GP2). However, it was taken care that none of the included loops lead to collisions with the remaining part of the model. Because the focus within the study is the binding mode of selected compounds in the active state hH_4R, the G$\beta\gamma$ was included, as given in the 3SN6 crystal. The resulting complex was energetically minimized. Afterward, the minimized receptor model was embedded into a POPC lipid bilayer, as described previously.[84] Intracellular and extracellular water, as well as an appropriate number of sodium and chloride ions, were added into the simulation box, and the molecular dynamic simulations, using GROMACS 4.0.2 (http://www.gromacs.org), were performed as already described.[83] For the POPC lipid, the force field parameters of the online source (http://moose.bio.ucalgary.ca/index.php?page=Structures_and_Topologies) were used. Subsequent to a 5 ns equilibration phase for each system (force constants (250 kJ/(mol nm^2) for the first 2.5 ns and 100 kJ/(mol nm^2) for the second 2.5 ns) were put onto the backbone atoms of the TM domains of hH_4R), the 15 ns productive phases were performed.

■ ASSOCIATED CONTENT

Supporting Information

The Supporting Information is available free of charge on the ACS Publications website at DOI: 10.1021/acs.jmedchem.6b00120. CCDC 965185 and CCDC 965186 contain the supplementary crystallographic data for *cis*-(1*R*,3*S*)-**53**·H_2O and *cis*-(1*R*,3*S*)-**17**·2HCl, respectively (available free of charge at The Cambridge Crystallographic Data Centre via www.ccdc.cam.ac.uk/data_request/cif).

Synthetic procedures and analytical data for compounds **16**–**17**, **31**–**36**, **43**, **44**, **62**–**65**, HPLC purity data of all target compounds, agonism of enantiomers in the luciferase reporter gene assay at the mH_4R, and alignment of Gαs and Gαi2 (PDF)

Molecular formula strings (CSV)

■ AUTHOR INFORMATION

Corresponding Author

* Phone: (+49)941-9434827. Fax: (+49)941-9434820. E-mail: armin.buschauer@ur.de.

Notes

The authors declare no competing financial interest.

■ ACKNOWLEDGMENTS

We are grateful to Maria Beer-Kroen, Gertraud Wilberg, Dr. Sebastian Wittmann, Helena Konkel, Dr. Manfred Zabel, and Nikola Kastner-Pustet for expert technical assistance, to Dr. Patrick Igel for helpful discussions and providing compounds **1** and [^{3}H]**60**, and to Edith Bartole and Dr. Paul Baumeister for resynthesis and pharmacological characterization of various reference compounds, including **1** and [^{3}H]**60**. This work was supported by the Graduate Training Programs GRK 760 and GRK 1910 ("Medicinal Chemistry of Selective GPCR Ligands") of the Deutsche Forschungsgemeinschaft.

■ ABBREVIATIONS USED

α, intrinsic activity (corresponding to the maximal response (E_{max}) in the context of functional pharmacological data); aq, aqueous; Boc, *tert*-butoxycarbonyl; DCM, dichloromethane; DMF, dimethylformamide; DMSO, dimethyl sulfoxide; EDTA, ethylenediaminetetraacetic acid; EI-MS, electron-impact ionization mass spectrometry; ES-MS, electrospray ionization mass spectrometry; GTP, guanosine 5′-triphosphate; GTPγS,

DOI: 10.1021/acs.jmedchem.6b00120
J. Med. Chem. XXXX, XXX, XXX–XXX

guanosine 5′-thiotriphosphate; GPCR, G protein-coupled receptor; $G\beta_1\gamma_2$, G protein β_1- and γ_2-subunit; $G\alpha_i$, α-subunit of the G_i protein that mediates inhibition of adenylyl cyclase; HMBC, heteronuclear multiple bond correlation; H_1R, histamine H_1 receptor; H_2R, histamine H_2 receptor; H_3R, histamine H_3 receptor; H_4R, histamine H_4 receptor; hH_1R, human H_1R; hH_2R, human H_2R; $hH_2R\text{-}Gs_{\alpha S}$, fusion protein of the hH_2R and the short splice variant of Gs_α; hH_3R, human H_3R; hH_4R, human H_4R; mH_4R, mouse H_4R; HR-MS, high resolution mass spectrometry; HSQC, heteronuclear single quantum coherence; LSI-MS, liquid-secondary-ion mass spectrometry; NOESY, nuclear Overhauser enhancement spectroscopy; RGS, regulator of G protein signaling proteins; SEM, standard error of the mean; TM, transmembrane domain of a GPCR; THF, tetrahydrofuran

REFERENCES

(1) Nguyen, T.; Shapiro, D. A.; George, S. R.; Setola, V.; Lee, D. K.; Cheng, R.; Rauser, L.; Lee, S. P.; Lynch, K. R.; Roth, B. L.; O'Dowd, B. F. Discovery of a novel member of the histamine receptor family. *Mol. Pharmacol.* **2001**, *59*, 427−433.

(2) Oda, T.; Morikawa, N.; Saito, Y.; Masuho, Y.; Matsumoto, S. Molecular cloning and characterization of a novel type of histamine receptor preferentially expressed in leukocytes. *J. Biol. Chem.* **2000**, *275*, 36781−36786.

(3) Nakamura, T.; Itadani, H.; Hidaka, Y.; Ohta, M.; Tanaka, K. Molecular cloning and characterization of a new human histamine receptor, hH_4R. *Biochem. Biophys. Res. Commun.* **2000**, *279*, 615−620.

(4) Zhu, Y.; Michalovich, D.; Wu, H.-L.; Tan, K. B.; Dytko, G. M.; Mannan, I. J.; Boyce, R.; Alston, J.; Tierney, L. A.; Li, X.; Herrity, N. C.; Vawter, L.; Sarau, H. M.; Ames, R. S.; Davenport, C. M.; Hieble, J. P.; Wilson, S.; Bergsma, D. J.; Fitzgerald, L. R. Cloning, expression, and pharmacological characterization of a novel human histamine receptor. *Mol. Pharmacol.* **2001**, *59*, 434−441.

(5) Morse, K. L.; Behan, J.; Laz, T. M.; West, R. E., Jr.; Greenfeder, S. A.; Anthes, J. C.; Umland, S.; Wan, Y.; Hipkin, R. W.; Gonsiorek, W.; Shin, N.; Gustafson, E. L.; Qiao, X.; Wang, S.; Hedrick, J. A.; Greene, J.; Bayne, M.; Monsma, F. J., Jr. Cloning and characterization of a novel human histamine receptor. *J. Pharmacol. Exp. Ther.* **2001**, *296*, 1058−1066.

(6) Liu, C.; Ma, X.-J.; Jiang, X.; Wilson, S. J.; Hofstra, C. L.; Blevitt, J.; Pyati, J.; Li, X.; Chai, W.; Carruthers, N.; Lovenberg, T. W. Cloning and pharmacological characterization of a fourth histamine receptor (H_4) expressed in bone marrow. *Mol. Pharmacol.* **2001**, *59*, 420−426.

(7) Coge, F.; Guenin, S.-P.; Rique, H.; Boutin, J. A.; Galizzi, J.-P. Structure and expression of the human histamine H_4-receptor gene. *Biochem. Biophys. Res. Commun.* **2001**, *284*, 301−309.

(8) de Esch, I. J.; Thurmond, R. L.; Jongejan, A.; Leurs, R. The histamine H4 receptor as a new therapeutic target for inflammation. *Trends Pharmacol. Sci.* **2005**, *26*, 462−469.

(9) Lim, H. D.; Smits, R. A.; Leurs, R.; De Esch, I. J. The emerging role of the histamine H_4 receptor in anti-inflammatory therapy. *Curr. Top. Med. Chem.* **2006**, *6*, 1365−1373.

(10) Reher, T. M.; Buschauer, A.; Neumann, D.; Seifert, R. Incomplete activation of human eosinophils via the histamine H_4-receptor: evidence for ligand-specific receptor conformations. *Biochem. Pharmacol.* **2012**, *84*, 192−203.

(11) Salcedo, C.; Pontes, C.; Merlos, M. Is the H4 receptor a new drug target for allergies and asthma? *Front. Biosci., Elite Ed.* **2013**, *5*, 178−187.

(12) Smits, R. A.; Leurs, R.; de Esch, I. J. P. Major advances in the development of histamine H4 receptor ligands. *Drug Discovery Today* **2009**, *14*, 745−753.

(13) Thurmond, R. L.; Gelfand, E. W.; Dunford, P. J. The role of histamine H1 and H4 receptors in allergic inflammation: the search for new antihistamines. *Nat. Rev. Drug Discovery* **2008**, *7*, 41−53.

(14) Yu, F.; Bonaventure, P.; Thurmond, R. L. The future antihistamines: histamine H3 and H4 receptor ligands. *Adv. Exp. Med. Biol.* **2010**, *709*, 125−140.

(15) Zhang, M.; Venable, J. D.; Thurmond, R. L. The histamine H4 receptor in autoimmune disease. *Expert Opin. Invest. Drugs* **2006**, *15*, 1443−1452.

(16) Panula, P.; Chazot, P. L.; Cowart, M.; Gutzmer, R.; Leurs, R.; Liu, W. L.; Stark, H.; Thurmond, R. L.; Haas, H. L. International Union of Basic and Clinical Pharmacology. XCVIII. Histamine receptors. *Pharmacol. Rev.* **2015**, *67*, 601−655.

(17) Cowden, J. M.; Zhang, M.; Dunford, P. J.; Thurmond, R. L. The histamine H4 receptor mediates inflammation and pruritus in Th2-dependent dermal inflammation. *J. Invest. Dermatol.* **2010**, *130*, 1023−1033.

(18) Igel, P.; Dove, S.; Buschauer, A. Histamine H_4 receptor agonists. *Bioorg. Med. Chem. Lett.* **2010**, *20*, 7191−7199.

(19) Marson, C. M. Targeting the histamine H4 receptor. *Chem. Rev.* **2011**, *111*, 7121−7156.

(20) Kiss, R.; Keseru, G. M. Novel histamine H4 receptor ligands and their potential therapeutic applications: an update. *Expert Opin. Ther. Pat.* **2014**, *24*, 1185−1197.

(21) Schreeb, A.; Łażewska, D.; Dove, S.; Buschauer, A.; Kieć-Kononiwcz, K.; Stark, H. Histamine H_4 receptor ligands. In *Histamine H4 Receptor: A Novel Drug Target in Immunoregulation and Inflammation*, Stark, H., Ed.; Versita: London, 2013; pp 21−62.

(22) Kollmeier, A.; Francke, K.; Chen, B.; Dunford, P. J.; Greenspan, A. J.; Xia, Y.; Xu, X. L.; Zhou, B.; Thurmond, R. The H4 receptor antagonist, JNJ 39758979, is effective in reducing histamine-induced pruritus in a randomized clinical study in healthy subjects. *J. Pharmacol. Exp. Ther.* **2014**, *350*, 181−187.

(23) Thurmond, R. L.; Chen, B.; Dunford, P. J.; Greenspan, A. J.; Karlsson, L.; La, D.; Ward, P.; Xu, X. L. Clinical and preclinical characterization of the histamine H(4) receptor antagonist JNJ-39758979. *J. Pharmacol. Exp. Ther.* **2014**, *349*, 176−184.

(24) Cowden, J. M.; Yu, F.; Banie, H.; Farahani, M.; Ling, P.; Nguyen, S.; Riley, J. P.; Zhang, M.; Zhu, J.; Dunford, P. J.; Thurmond, R. L. The histamine H4 receptor mediates inflammation and Th17 responses in preclinical models of arthritis. *Ann. Rheum. Dis.* **2014**, *73*, 600−608.

(25) Werner, K.; Neumann, D.; Buschauer, A.; Seifert, R. No evidence for histamine H4-receptor in human monocytes. *J. Pharmacol. Exp. Ther.* **2014**, *351*, 519−526.

(26) Feliszek, M.; Speckmann, V.; Schacht, D.; von Lehe, M.; Stark, H.; Schlicker, E. A search for functional histamine H4 receptors in the human, guinea pig and mouse brain. *Naunyn-Schmiedeberg's Arch. Pharmacol.* **2015**, *388*, 11−17.

(27) Schneider, E. H.; Neumann, D.; Seifert, R. Histamine H4-receptor expression in the brain? *Naunyn-Schmiedeberg's Arch. Pharmacol.* **2015**, *388*, 5−9.

(28) Hough, L. B. Genomics meets histamine receptors: new subtypes, new receptors. *Mol. Pharmacol.* **2001**, *59*, 415−419.

(29) Liu, C.; Wilson, S. J.; Kuei, C.; Lovenberg, T. W. Comparison of human, mouse, rat, and guinea pig histamine H4 receptors reveals substantial pharmacological species variation. *J. Pharmacol. Exp. Ther.* **2001**, *299*, 121−130.

(30) Lim, H. D.; de Graaf, C.; Jiang, W.; Sadek, P.; McGovern, P. M.; Istyastono, E. P.; Bakker, R. A.; de Esch, I. J.; Thurmond, R. L.; Leurs, R. Molecular determinants of ligand binding to H4R species variants. *Mol. Pharmacol.* **2010**, *77*, 734−743.

(31) Schnell, D.; Brunskole, I.; Ladova, K.; Schneider, E.; Igel, P.; Dove, S.; Buschauer, A.; Seifert, R. Expression and functional properties of canine, rat, and murine histamine H_4 receptors in Sf9 insect cells. *Naunyn-Schmiedeberg's Arch. Pharmacol.* **2011**, *383*, 457−470.

(32) Strasser, A.; Wittmann, H.-J.; Buschauer, A.; Schneider, E. H.; Seifert, R. Species-dependent activities of GPCR ligands: lessons from histamine receptor orthologs. *Trends Pharmacol. Sci.* **2013**, *34*, 13−32.

(33) Nordemann, U.; Wifling, D.; Schnell, D.; Bernhardt, G.; Stark, H.; Seifert, R.; Buschauer, A. Luciferase reporter gene assay on human,

DOI: 10.1021/acs.jmedchem.6b00120
J. Med. Chem. XXXX, XXX, XXX−XXX

murine and rat histamine H_4 receptor orthologs: correlations and discrepancies between distal and proximal readouts. *PLoS One* **2013**, *8*, e73961.
(34) Neumann, D.; Beermann, S.; Seifert, R. Does the histamine H-4 receptor have a pro- or anti-inflammatory role in murine bronchial asthma? *Pharmacology* **2010**, *85*, 217−223.
(35) Seifert, R.; Schneider, E. H.; Dove, S.; Brunskole, I.; Neumann, D.; Strasser, A.; Buschauer, A. Paradoxical stimulatory effects of the "standard" histamine H4-receptor antagonist JNJ7777120: The H4-receptor joins the club of 7TM receptors exhibiting functional selectivity. *Mol. Pharmacol.* **2011**, *79*, 631−638.
(36) Tichenor, M. S.; Thurmond, R. L.; Venable, J. D.; Savall, B. M. Functional profiling of 2-aminopyrimidine histamine H4 receptor modulators. *J. Med. Chem.* **2015**, *58*, 7119−7127.
(37) Igel, P.; Geyer, R.; Strasser, A.; Dove, S.; Seifert, R.; Buschauer, A. Synthesis and structure activity relationships of cyanoguanidine-type and structurally related histamine H_4 receptor agonists. *J. Med. Chem.* **2009**, *52*, 6297−6313.
(38) Lim, H. D.; van Rijn, R. M.; Ling, P.; Bakker, R. A.; Thurmond, R. L.; Leurs, R. Evaluation of histamine H_1−, H_2−, and H_3-receptor ligands at the human histamine H_4 receptor: identification of 4-methylhistamine as the first potent and selective H_4 receptor agonist. *J. Pharmacol. Exp. Ther.* **2005**, *314*, 1310−1321.
(39) Geyer, R.; Kaske, M.; Baumeister, P.; Buschauer, A. Synthesis and functional characterization of imbutamine analogs as histamine H_3 and H_4 receptor ligands. *Arch. Pharm. (Weinheim, Ger.)* **2014**, *347*, 77−88.
(40) Harusawa, S.; Imazu, T.; Takashima, S.; Araki, L.; Ohishi, H.; Kurihara, T.; Sakamoto, Y.; Yamamoto, Y.; Yamatodani, A. Synthesis of 4(5)-[5-(aminomethyl)tetrahydrofuran-2-yl- or 5-(aminomethyl)-2,5-dihydrofuran-2-yl]imidazoles by efficient use of a PhSe group: application to novel histamine H_3-ligands. *J. Org. Chem.* **1999**, *64*, 8608−8615.
(41) Harusawa, S.; Imazu, T.; Takashima, S.; Araki, L.; Ohishi, H.; Kurihara, T.; Yamamoto, Y.; Yamatodani, A. Synthesis of imifuramine and its stereoisomers exhibiting histamine H3-agonistic activity. *Tetrahedron Lett.* **1999**, *40*, 2561−2564.
(42) Hashimoto, T.; Harusawa, S.; Araki, L.; Zuiderveld, O. P.; Smit, M. J.; Imazu, T.; Takashima, S.; Yamamoto, Y.; Sakamoto, Y.; Kurihara, T.; Leurs, R.; Bakker, R. A.; Yamatodani, A. A selective human H_4-receptor agonist: (−)-2-cyano-1-methyl-3-(2*R*,5*R*)-5-[1*H*-imidazol-4(5)-yl]tetrahydrofuran-2-ylmethylguanidine. *J. Med. Chem.* **2003**, *46*, 3162−3165.
(43) Watanabe, M.; Kazuta, Y.; Hayashi, H.; Yamada, S.; Matsuda, A.; Shuto, S. Stereochemical diversity-oriented conformational restriction strategy. Development of potent histamine H_3 and/or H_4 receptor antagonists with an imidazolylcyclopropane structure. *J. Med. Chem.* **2006**, *49*, 5587−5596.
(44) Geyer, R.; Buschauer, A. Synthesis and histamine H_3 and H_4 receptor activity of conformationally restricted cyanoguanidines related to UR-PI376. *Arch. Pharm. (Weinheim, Ger.)* **2011**, *344*, 775−842.
(45) Zimmermann, F.; Meux, E.; Mieloszynski, J.-L.; Lecuire, J.-M.; Oget, N. Ruthenium catalysed oxidation without CCl_4 of oleic acid, other monoenic fatty acids and alkenes. *Tetrahedron Lett.* **2005**, *46*, 3201−3203.
(46) Yoon, N. M.; Pak, C. S.; Brown, H. C.; Krishnamurthy, S.; Stocky, T. P. Selective reductions. 19. Rapid reaction of carboxylic-acids with borane-tetrahydrofuran - remarkably convenient procedure for selective conversion of carboxylic-acids to corresponding alcohols in presence of other functional groups. *J. Org. Chem.* **1973**, *38*, 2786−2792.
(47) Birch, S. F.; Dean, R. A. 502. The configurations of the isomeric forms of 1:3-dimethylcyclopentane. *J. Chem. Soc.* **1953**, 2477−2481.
(48) Omura, K.; Swern, D. Oxidation of alcohols by "activated" dimethyl sulfoxide. a preparative, steric and mechanistic study. *Tetrahedron* **1978**, *34*, 1651−1660.
(49) Horne, D. A.; Yakushijin, K.; Buechi, G. A two-step synthesis of imidazoles from aledhydes via 4-tosyloxazolines. *Heterocycles* **1994**, *39*, 139−153.
(50) Mitsunobu, O.; Yamada, M.; Mukaiyama, T. Preparation of esters of phosphoric acid by the reaction of trivalent phosphorus compounds with diethyl azodicarboxylate in the presence of alcohols. *Bull. Chem. Soc. Jpn.* **1967**, *40*, 935−939.
(51) Buschauer, A. Synthesis and pharmacological activity of arylmethylthioethylguanidines. *Arzneim.-Forsch.* **1987**, *37*, 1008−1012.
(52) Webb, R. L.; Labaw, C. S. Diphenyl cyanocarbonimidate. A versatile synthon for the construction of heterocyclic systems. *J. Heterocycl. Chem.* **1982**, *19*, 1205−1206.
(53) Webb, R. L.; Eggleston, D. S.; Labaw, C. S.; Lewis, J. J.; Wert, K. Diphenyl cyancarbonimidate and dichlorodiphenoxymethane as synthons for the construction of heterocyclic systems of medicinal interest. *J. Heterocycl. Chem.* **1987**, *24*, 275−278.
(54) Chênevert, R.; Martin, R. Enantioselective synthesis of (+) and (−)-cis-3-aminocyclo-pentanecarboxylic acids by enzymatic asymmetrization. *Tetrahedron: Asymmetry* **1992**, *3*, 199−200.
(55) Chênevert, R.; Lavoie, M.; Courchesne, G.; Martin, R. Chemoenzymatic enantioselective synthesis of amidinomycin. *Chem. Lett.* **1994**, *23*, 93−96.
(56) Hronowski, L. J. J.; Szarek, W. A. Synthesis of cyclopentane analogs of 1-(2',3'-dideoxy-beta -glycero-pentofuranosyl)pyrimidine nucleosides. *Can. J. Chem.* **1988**, *66*, 61−70.
(57) Jones, J. B.; Hinks, R. S.; Hultin, P. G. Enzymes in organic synthesis. 33. Stereoselective pig-liver esterase-catalyzed hydrolyses of meso-cyclopentyl-1,3-diesters, tetrahydrofuranyl-1,3-diesters, and tetrahydrothiophenyl-1,3-diesters. *Can. J. Chem.* **1985**, *63*, 452−456.
(58) Lim, H. D.; Smits, R. A.; Bakker, R. A.; van Dam, C. M.; de Esch, I. J.; Leurs, R. Discovery of S-(2-guanidylethyl)-isothiourea (VUF 8430) as a potent nonimidazole histamine H4 receptor agonist. *J. Med. Chem.* **2006**, *49*, 6650−6651.
(59) Igel, P.; Schnell, D.; Bernhardt, G.; Seifert, R.; Buschauer, A. Tritium-labeled N^1-[3-(1*H*-imidazol-4-yl)propyl]-N^2-propionylguanidine ([^{3}H]UR-PI294), a high-affinity histamine H_3 and H_4 receptor radioligand. *ChemMedChem* **2009**, *4*, 225−231.
(60) Igel, P.; Schneider, E.; Schnell, D.; Elz, S.; Seifert, R.; Buschauer, A. N^G-Acylated imidazolylpropylguanidines as potent histamine H_4 receptor agonists: selectivity by variation of the N^G-substituent. *J. Med. Chem.* **2009**, *52*, 2623−2627.
(61) Xie, S.-X.; Ghorai, P.; Ye, Q.-Z.; Buschauer, A.; Seifert, R. Probing ligand-specific histamine H_1- and H_2-receptor conformations with N^G-acylated imidazolylpropylguanidines. *J. Pharmacol. Exp. Ther.* **2006**, *317*, 139−146.
(62) Kagermeier, N.; Werner, K.; Keller, M.; Baumeister, P.; Bernhardt, G.; Seifert, R.; Buschauer, A. Dimeric carbamoylguanidine-type histamine H2 receptor ligands: A new class of potent and selective agonists. *Bioorg. Med. Chem.* **2015**, *23*, 3957−3969.
(63) Wifling, D.; Löffel, K.; Nordemann, U.; Strasser, A.; Bernhardt, G.; Dove, S.; Seifert, R.; Buschauer, A. Molecular determinants for the high constitutive activity of the human histamine H_4 receptor: Functional studies on orthologs and mutants. *Br. J. Pharmacol.* **2015**, *172*, 785−798.
(64) Yu, F.; Wolin, R. L.; Wei, J.; Desai, P. J.; McGovern, P. M.; Dunford, P. J.; Karlsson, L.; Thurmond, R. L. Pharmacological characterization of oxime agonists of the histamine H_4 receptor. *J. Recept., Ligand Channel Res.* **2010**, *3*, 37−49.
(65) Davey, D. D.; Lumma, W. C. Convenient synthesis of 4-methylhistamine and racemic α,4-dimethylhistamine and α,4-dimethylhistidine. *J. Org. Chem.* **1989**, *54*, 3211−3213.
(66) Lange, J. H. M.; Wals, H. C.; den Hoogenband, A. v.; de Kuilen, A. v.; den Hartog, J. A. J. Two novel syntheses of the histamine H3 antagonist thioperamide. *Tetrahedron* **1995**, *51*, 13447−13454.
(67) Jablonowski, J. A.; Grice, C. A.; Chai, W.; Dvorak, C. A.; Venable, J. D.; Kwok, A. K.; Ly, K. S.; Wei, J.; Baker, S. M.; Desai, P. J.; Jiang, W.; Wilson, S. J.; Thurmond, R. L.; Karlsson, L.; Edwards, J. P.; Lovenberg, T. W.; Carruthers, N. I. The first potent and selective non-

DOI: 10.1021/acs.jmedchem.6b00120
J. Med. Chem. XXXX, XXX, XXX−XXX

imidazole human histamine H_4 receptor antagonists. *J. Med. Chem.* **2003**, *46*, 3957−3960.
(68) Walseth, T. F.; Johnson, R. A. The enzymatic preparation of [α-^{32}P] nucleoside triphosphates, cyclic [^{32}P] AMP, and cyclic [^{32}P] GMP. *Biochim. Biophys. Acta, Nucleic Acids Protein Synth.* **1979**, *562*, 11−31.
(69) Asano, T.; Pedersen, S. E.; Scott, C. W.; Ross, E. Reconstitution of catecholamine-stimulated binding of guanosine 5′-O-(3-thiotriphosphate) to the stimulatory GTP-binding protein of adenylate cyclase. *Biochemistry* **1984**, *23*, 5460−5467.
(70) Hilf, G.; Gierschik, P.; Jakobs, K. H. Muscarinic acetylcholine receptor-stimulated binding of guanosine 5′-O-(3-thiotriphosphate) to guanine-nucleotide-binding proteins in cardiac membranes. *Eur. J. Biochem.* **1989**, *186*, 725−731.
(71) Houston, C.; Wenzel-Seifert, K.; Bürckstümmer, T.; Seifert, R. The human histamine H_2-receptor couples more eficiently to Sf9 insect cell Gs-proteins than to insect cell G_q-proteins: limitations of Sf9 cells for the analysis of receptor/G_q-protein coupling. *J. Neurochem.* **2002**, *80*, 678−696.
(72) Wenzel-Seifert, K.; Kelley, M. T.; Buschauer, A.; Seifert, R. Similar apparent constitutive activity of human histamine H_2-receptor fused to long and short splice variants of Gs_α. *J. Pharmacol. Exp. Ther.* **2001**, *299*, 1013−1020.
(73) Rouleau, A.; Ligneau, X.; Tardivel-Lacombe, J.; Morisset, S.; Gbahou, F.; Schwartz, J. C.; Arrang, J. M. Histamine H_3-receptor-mediated [^{35}S]GTPγS binding: evidence for constitutive activity of the recombinant and native rat and human H_3 receptors. *Br. J. Pharmacol.* **2002**, *135*, 383−392.
(74) Schnell, D.; Burleigh, K.; Trick, J.; Seifert, R. No evidence for functional selectivity of proxyfan at the human histamine H_3 receptor coupled to defined Gi/Go protein heterotrimers. *J. Pharmacol. Exp. Ther.* **2010**, *332*, 996−1005.
(75) Schneider, E. H.; Schnell, D.; Papa, D.; Seifert, R. High constitutive activity and a G-protein-independent high-affinity state of the human histamine H_4-receptor. *Biochemistry* **2009**, *48*, 1424−1438.
(76) Ghorai, P.; Kraus, A.; Birnkammer, T.; Geyer, R.; Bernhardt, G.; Dove, S.; Seifert, R.; Elz, S.; Buschauer, A. Chiral N^G-acylated hetarylpropylguanidine-type histamine H_2 receptor agonists do not show significant stereoselectivity. *Bioorg. Med. Chem. Lett.* **2010**, *20*, 3173−3176.
(77) Ghorai, P.; Kraus, A.; Keller, M.; Goette, C.; Igel, P.; Schneider, E.; Schnell, D.; Bernhardt, G.; Dove, S.; Zabel, M.; Elz, S.; Seifert, R.; Buschauer, A. Acylguanidines as Bioisosteres of Guanidines: N^G-Acylated imidazolylpropylguanidines, a new class of histamine H_2 receptor agonists. *J. Med. Chem.* **2008**, *51*, 7193−7204.
(78) Kelley, M. T.; Bürckstümmer, T.; Wenzel-Seifert, K.; Dove, S.; Buschauer, A.; Seifert, R. Distinct interaction of human and guinea pig histamine H_2-Receptor with guanidine-type agonists. *Mol. Pharmacol.* **2001**, *60*, 1210−1225.
(79) Seifert, R.; Wenzel-Seifert, K.; Bürckstümmer, T.; Pertz, H. H.; Schunack, W.; Dove, S.; Buschauer, A.; Elz, S. Multiple differences in agonist and antagonist pharmacology between human and guinea pig histamine H_1-receptor. *J. Pharmacol. Exp. Ther.* **2003**, *305*, 1104−1115.
(80) Seifert, R.; Wenzel-Seifert, K.; Gether, U.; Kobilka, B. K. Functional differences between full and partial agonists: evidence for ligand-specific receptor conformations. *J. Pharmacol. Exp. Ther.* **2001**, *297*, 1218−1226.
(81) Cheng, Y.-C.; Prusoff, W. H. Relationship between the inhibition constant (K_I) and the concentration of inhibitor which causes 50% inhibition (I_{50}) of an enzymatic reaction. *Biochem. Pharmacol.* **1973**, *22*, 3099−3108.
(82) Shimamura, T.; Shiroishi, M.; Weyand, S.; Tsujimoto, H.; Winter, G.; Katritch, V.; Abagyan, R.; Cherezov, V.; Liu, W.; Han, G. W.; Kobayashi, T.; Stevens, R. C.; Iwata, S. Structure of the human histamine H1 receptor complex with doxepin. *Nature* **2011**, *475*, 65−70.
(83) Wittmann, H. J.; Seifert, R.; Strasser, A. Sodium binding to hH3R and hH4R - a molecular modeling study. *J. Mol. Model.* **2014**, *20*, 2394.
(84) Strasser, A.; Wittmann, H. J. Molecular modeling studies give hint for the existence of a symmetric hbeta(2)R-Galphabetagamma-homodimer. *J. Mol. Model.* **2013**, *19*, 4443−4457.
(85) Angel, T. E.; Chance, M. R.; Palczewski, K. Conserved waters mediate structural and functional activation of family A (rhodopsin-like) G protein-coupled receptors. *Proc. Natl. Acad. Sci. U. S. A.* **2009**, *106*, 8555−8560.
(86) Liu, W.; Chun, E.; Thompson, A. A.; Chubukov, P.; Xu, F.; Katritch, V.; Han, G. W.; Roth, C. B.; Heitman, L. H.; Ijzerman, A. P.; Cherezov, V.; Stevens, R. C. Structural basis for allosteric regulation of GPCRs by sodium ions. *Science* **2012**, *337*, 232−236.
(87) Schüttelkopf, A. W.; van Aalten, D. M. PRODRG: a tool for high-throughput crystallography of protein-ligand complexes. *Acta Crystallogr., Sect. D: Biol. Crystallogr.* **2004**, *60*, 1355−1363.
(88) Rasmussen, S. G.; DeVree, B. T.; Zou, Y.; Kruse, A. C.; Chung, K. Y.; Kobilka, T. S.; Thian, F. S.; Chae, P. S.; Pardon, E.; Calinski, D.; Mathiesen, J. M.; Shah, S. T.; Lyons, J. A.; Caffrey, M.; Gellman, S. H.; Steyaert, J.; Skiniotis, G.; Weis, W. I.; Sunahara, R. K.; Kobilka, B. K. Crystal structure of the beta2 adrenergic receptor-Gs protein complex. *Nature* **2011**, *477*, 549−555.
(89) Wall, M. A.; Coleman, D. E.; Lee, E.; Iniguez-Lluhi, J. A.; Posner, B. A.; Gilman, A. G.; Sprang, S. R. The structure of the G protein heterotrimer Gi alpha 1 beta 1 gamma 2. *Cell* **1995**, *83*, 1047−1058.

DOI: 10.1021/acs.jmedchem.6b00120
J. Med. Chem. XXXX, XXX, XXX−XXX